# 4. INTERMEDIATE FIELD TEST 2

This section presents information of INEL ISV Intermediate Field Test 2 and includes the specific objectives of the test, construction of the test pit, description and assessment of the data collected during process operations. Product durability data are presented in Section 5. Results of the test tracer study are presented in Section 6. And information from analytical modeling based on off-gassing is presented in Section 7.

## 4.1 Test 2 Objectives and Test Pit Overview

Test 2 was designed to test the ISV process under two conditions: stacked waste and high metal content waste. Stacked waste presents a potential challenge for the ISV process in that such a region may contain a reduced amount of soil relative to the waste fraction. Additionally, a stacked waste region could challenge the capability of the off-gas processing system if several containers are breached at about the same time.

High metal content waste may result in a challenge to the process because ISV is based on resistance heating, and metal shorting could interfere with this process. Previous testing indicated limitations on allowable metal content; however, this testing was conducted with fixed electrodes. The use of the EFS provides a potential method to allow processing of high metal waste because the electrode can be inserted or retracted from the melt based on changing melt electrical characteristics.

Several aspects of Test Pit 2 design should be noted. First, the particular configuration of the pit (stacked drums located over stacked boxes) does not represent a disposal practice that is known to have been used at the SDA. The test was designed to represent the two situations independently, first the stacked waste and then the high metal waste. Second, the high metal content was represented as a stacked box region in which scrap metal and fill dirt was placed in the boxes. The use of fill dirt in the boxes did not occur

as a disposal practice at the SDA. It is possible that some filling-in of void spaces may have occurred in SDA waste containers as containers deteriorated with time. This is supported by documented occurrences of subsidence (particularly in springtime) of the SDA overburden soil. For the purposes of the ISV Test Pit 2, the soil was added to the boxes to provide sufficient soil so that the effect of high metal content on process performance could be assessed.

## 4.2 Test Pit 2 Construction Details

Test Pit 2 consisted of approximately 0.9 m (3 ft) of soil underburden, 0.91 m (3 ft) of a stacked box region, 0.6 m (2 ft) of a three layered stacked can region, and 1.2 m (4 ft) of soil overburden. Test Pit 2 was originally constructed with 0.6 m (2 ft) of overburden; however, an additional 0.6 m (2 ft) of soil was added after the completion of Test 1. This additional soil was added to ensure an amount of molten glass was formed prior to encountering the stacked can waste region and be sufficient to maintain conductance between the electrodes. During the placement of the additional overburden, a single instrumented can was placed at an approximate 0.6 m (2 ft) depth. Figure 50 shows a schematic of the contents of Test Pit 2 with the hood in place. The number of cans of each waste type in each of the three can layers is presented in Table 9. Tables 10 and 11 provide summary information on pit waste material contents.

Test Pit 2 was constructed by laying the soil underburden, then placing the stacked boxes into the pit. The stacked cans were then placed and the overburden put on top. The stacked boxes containing scrap metal with added fill dirt were loaded onto pallets and lowered by crane into the pit. Each pallet supported 12 boxes. Figure 51 shows the placement of the stacked boxes into the pit. After the boxes had been placed approximately 2.5 to 5.1 cm (1 to 2 in.) of dirt was placed on top to cover the boxes prior to laying three layers of stacked cans. Figure 52 shows the completed bottom layer of cans. The cans containing the dysprosium oxide tracer were placed near the center of this layer.

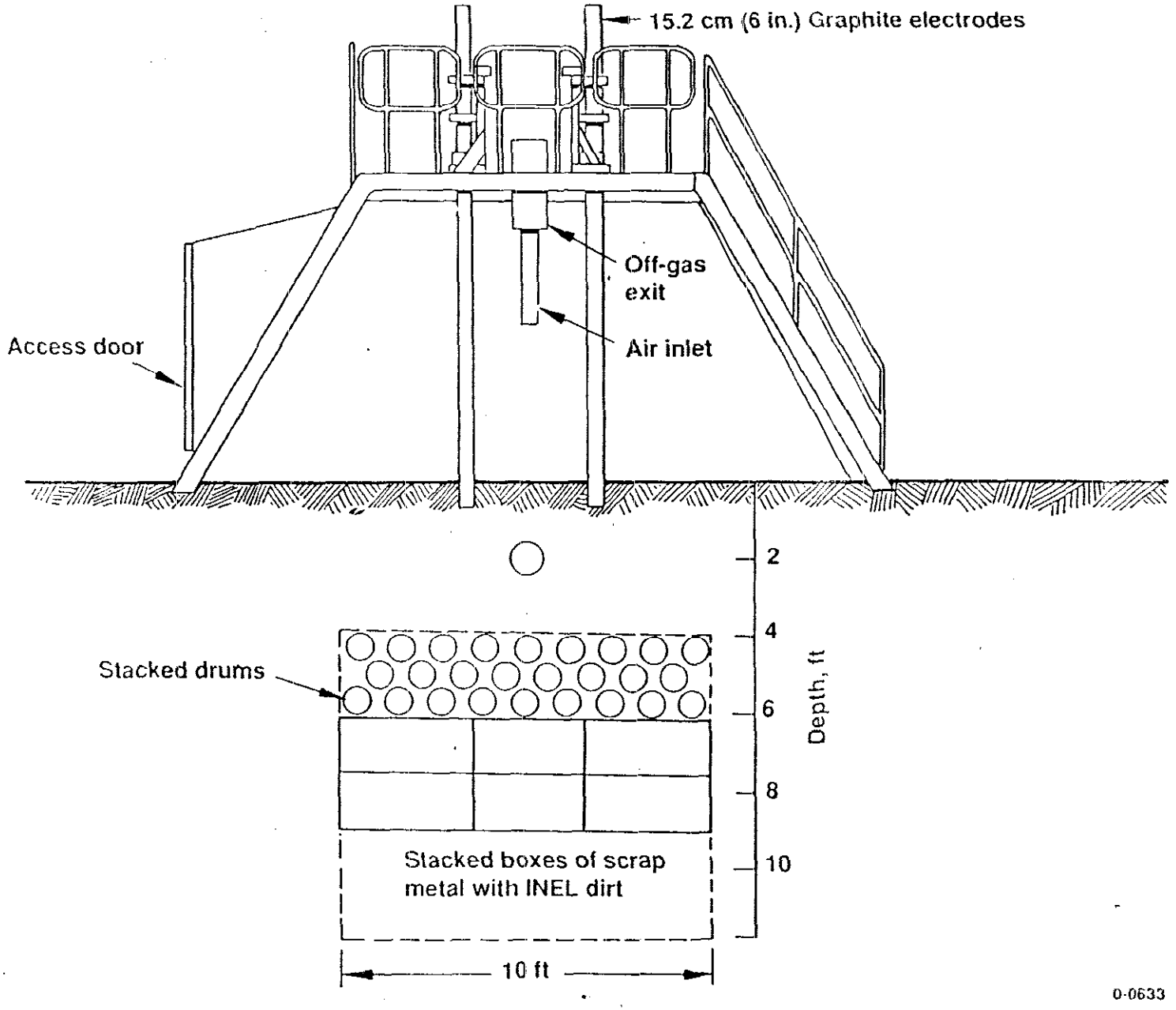


**Figure 50.** Schematic of Test Pit 2.

Table 9. Depth view of Test Pit 2[a]

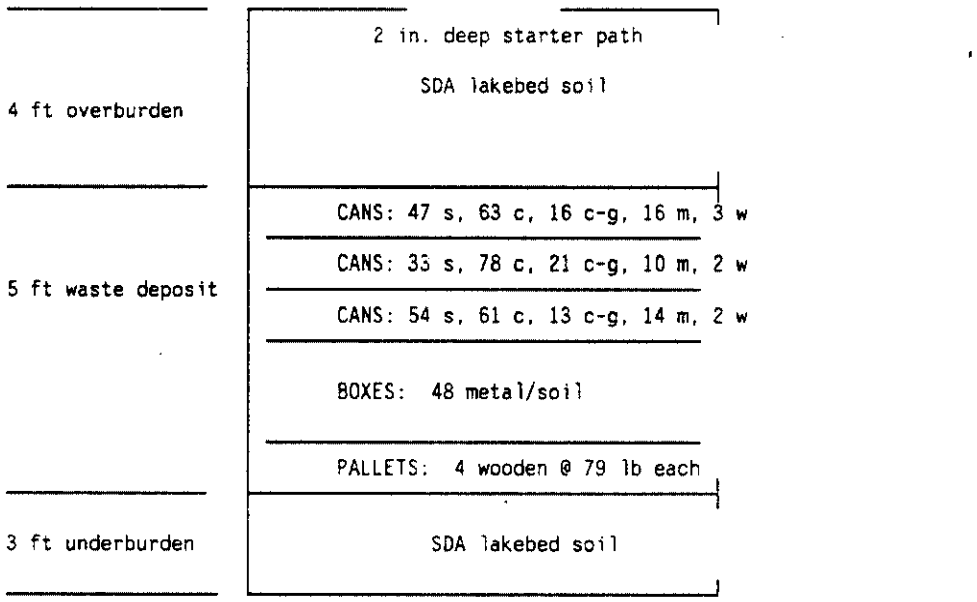


Where,

s is sludge cans

c is combustible cans

c-g is concrete/glass cans

m is metal cans

w is wood cans.

These cans contained the following, approximate amounts of material:

Sludge can (s) - 10.72 lb
(7.72 - H2O, 0.70 - FLOOR DRI, 2.307 - MICRO-CEL E)
Combustible can (c) - 3.96 lb (1.901 - Cloth, 2.059 - Paper)
Concrete/glass can (c-g) - 16.73 lb (12.0 - concrete, 4.73 - glass)
Metal can (m) - 6.58 lb (3.29 - carbon steel, 3.29 stainless steel)
Wood can (w) - 3.14 lb
Pallet - 79.0 lb of wood

Boxes contained the following, approximate amounts of material:

Metal/soil - 119.521 lb (50% carbon steel)
244.021 lb soil

a. Engineering Design File, EDF-ISV-034

Table 10. Test Pit 2 waste deposit material composition in pounds[a]

| MATERIALS | TOTAL | | ITEM WEIGHT | WASTE DEPOSIT LAYERS TOP CAN | MID CAN | BOT CAN | BOXES | PALLETS |
|---|---|---|---|---|---|---|---|---|
| COMBUSTIBLES: | 1,513.5 | | | | | | | |
| Cans: | | 813.5 | | | | | | |
| Paper | | | 411.50 | 128.24 | 159.13 | 124.13 | | |
| Cloth | | | 380.00 | 118.43 | 146.94 | 114.63 | | |
| Wood | | | 22.00 | 9.42 | 6.29 | 6.29 | | |
| Boxes: | | 700.0 | | | | | | |
| Cardboard | | | 384.00 | | | | 384.00 | |
| Pallet (wood) | | | 316.00 | | | | | 316.00 |
| SLUDGE: (cans only) | 1,436.5 | | | | | | | |
| Water | | 1,034.5 | 1,034.50 | 362.85 | 254.77 | 416.88 | | |
| Floor Dri | | 93.8 | 93.80 | 32.90 | 23.10 | 37.80 | | |
| Micro-Cel | | 308.2 | 308.20 | 108.10 | 75.90 | 124.20 | | |
| METALS: | 6,757.95 | | | | | | | |
| Cans: | | 1,020.95 | | | | | | |
| Stainless | | | 131.60 | 52.64 | 32.90 | 46.06 | | |
| Carbon Steel | | | 889.35 | 306.39 | 284.90 | 298.06 | | |
| Boxes: | | 5,737.0 | | | | | | |
| Stainless | | | 2,868.50 | | | | 2,868.50 | |
| Carbon Steel | | | 2,868.50 | | | | 2,868.50 | |
| CONCRETE/GLASS: | 12,549.50 | | | | | | | |
| Cans: | | 836.50 | | | | | | |
| Concrete | | | 600.00 | 192.00 | 252.00 | 156.00 | | |
| Glass | | | 236.50 | 75.68 | 99.33 | 61.49 | | |
| Boxes: | | | | | | | | |
| Soil | | 11,713.00 | 11,713.00 | | | | 11,713.00 | |
| TOTALS OF COLUMNS | 22,257.45 | | 22,257.45 | 1,386.65 | 1,335.26 | 1,385.54 | 17,834.00 | 316.00 |

a. Engineering Design File, EDF-ISV-034

Table 11. Test Pit 2 waste inventory

| Material | Mass (lb) | % of Total Mass |
|---|---|---|
| Combustible | 1514 | 2.5 |
| Sludge | | |
| Water | 1035 | 1.7 |
| FLOOR-DRI | 94 | 0.2 |
| MICRO-CELL E | 308 | 0.5 |
| Metal | 6758 | 11.2 |
| Glass | 237 | 0.4 |
| Concrete | 600 | 1.0 |
| Soil (excluding underburden) | 49,963 | 82.6 |
| Total | 60,509 | |

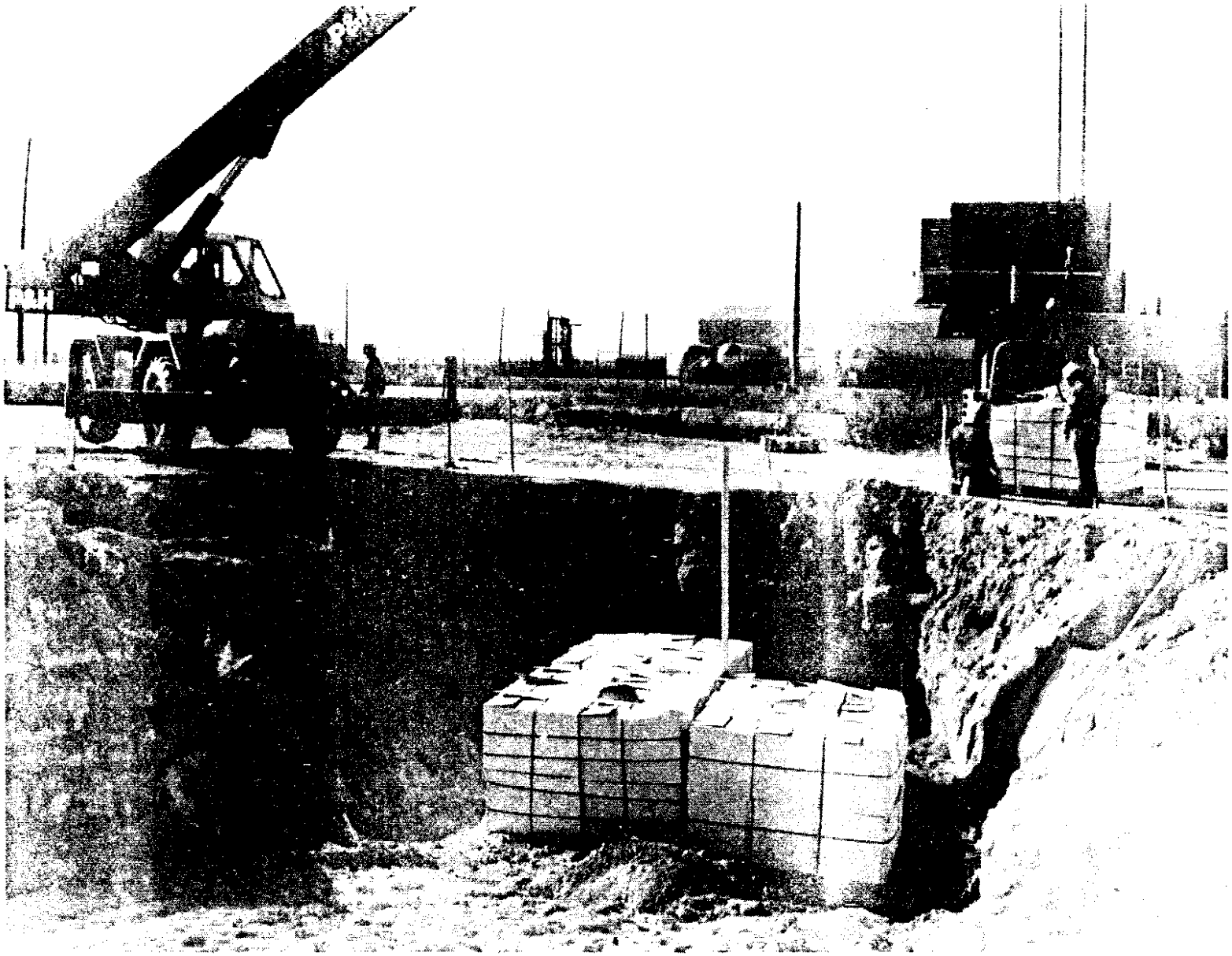

Figure 51. Placement of stacked boxes in Test Pit 2.

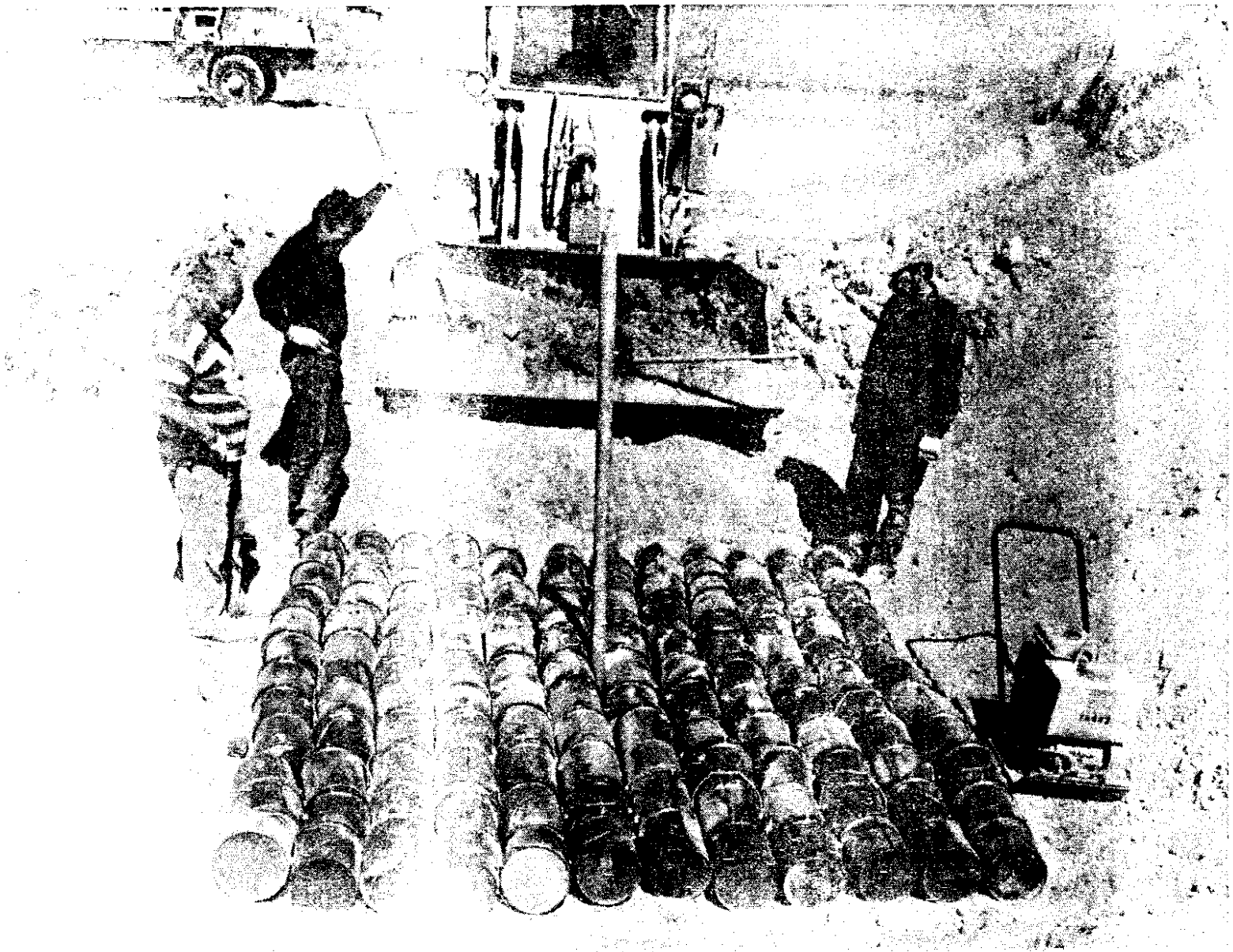

Figure 52. Bottom layer of cans in Test Pit 2.

During placement of the can layers, fill dirt was added to fill in the interstitial space between each layer, as shown in Figure 53. This figure also shows the placement of the horizontal array of thermocouples between the bottom and middle layers of cans. The middle layer of cans is shown in Figure 54. The dirt placed between the middle and top layers of cans is shown in Figure 55. Figure 56 shows the top layer of cans, and the final backfill is shown on Figure 57.

As indicated above, an additional 0.6 m (2 ft) of soil overburden was added to Test Pit 2 prior to conducting the second test. A single can containing approximately 1.8 kg (4 lb) of paper was added at the original ground surface layer [approximate 0.6 m (2 ft) depth after the additional overburden was added]. This can was instrumented with a type K thermocouple and a pressure transducer and was placed in order to gather pressure and temperature data from a single representative can during processing.

Two additional arrays of type K thermocouples were placed in Test Pit 2. A vertical array of 16 thermocouples was placed starting at approximately 15 cm (6 in.) from original ground level, with thermocouples spaced every 15 cm (6 in.) apart. After the addition of the extra 0.6 m (2 ft) of soil overburden, the first thermocouple was at approximately 0.76 m (2.5 ft) depth. The horizontal array of nine thermocouples was placed between the second and third layer of stacked cans as measured from the top of the test pit. These thermocouple arrays were placed using the same type of connecting wire as was used in Test Pit 1. However, after the failure of the Test Pit 1 thermocouples, it was decided to replace the connecting wire for the Test Pit 2 arrays. A trench was excavated to the point of connection and the wire replaced.

## 4.3 Operational Changes for Test 2

Following an evaluation of Test 1, several equipment and operational changes were initiated for Test 2. These changes were designed to gain additional data from the test and to remedy the key operational difficulties identified in Test 1; the changes implemented for the Test 2 are listed below.

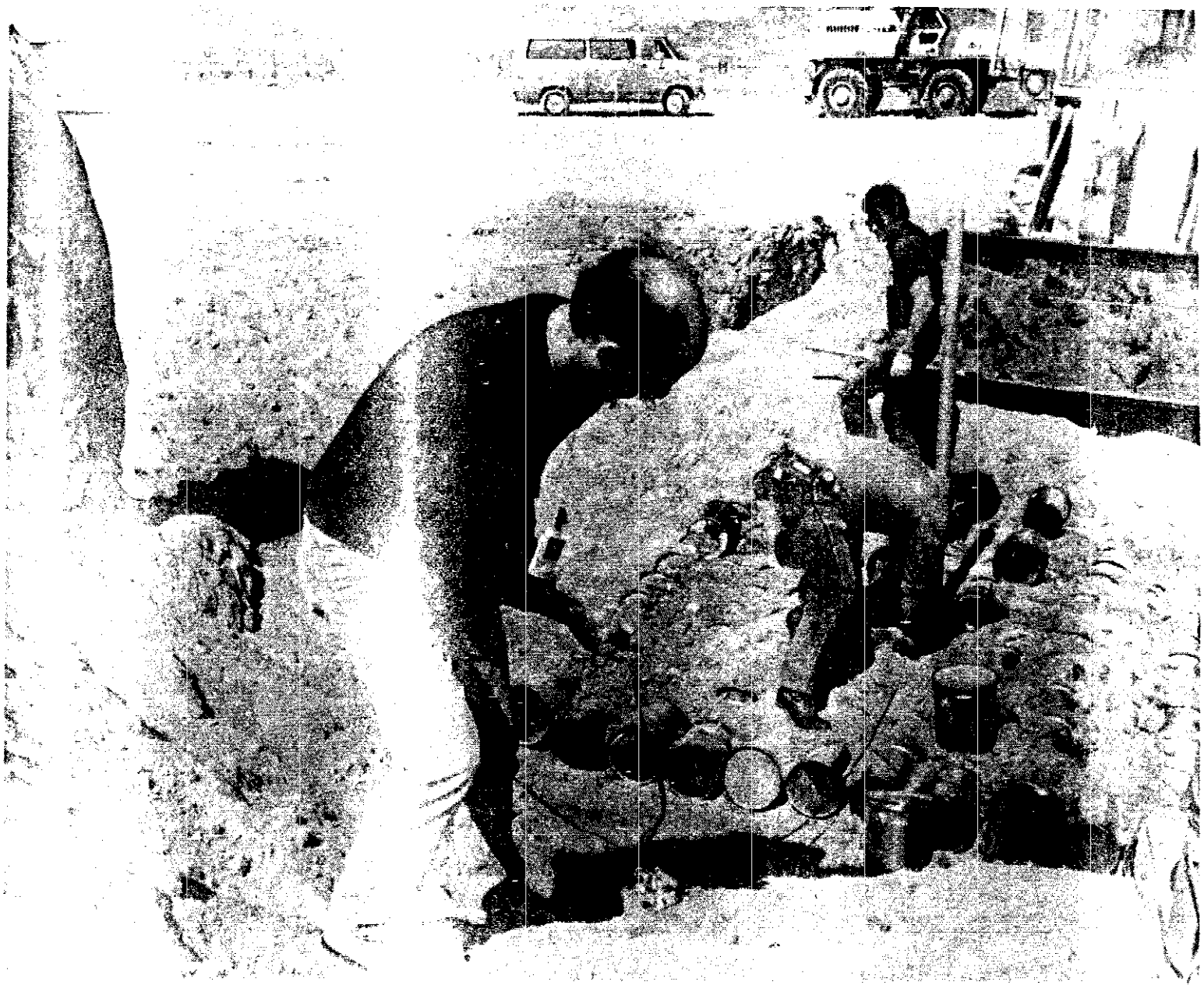

**Figure 53.** Placement of fill dirt between can layers in Test Pit 2.

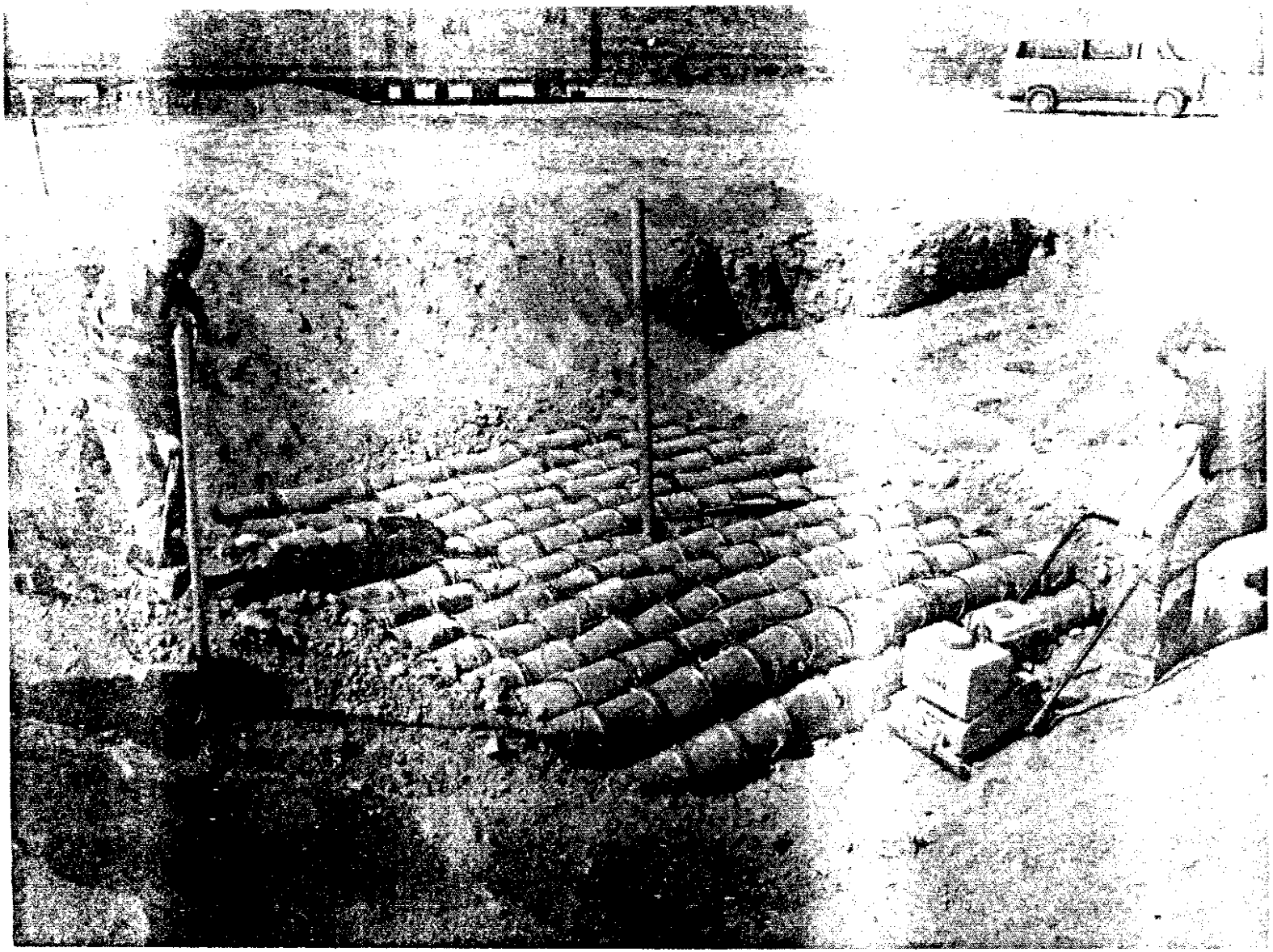

**Figure 54.** Placement of middle layer of cans in Test Pit 2.

Figure 55. Dirt placed between middle and top layers of cans in Test Pit 2.

Figure 56. Placement of top layer of cans in Test Pit 2

**Figure 57.** Final backfill for Test Pit 2.

- The electrodes were not coated with the silica-based coating as in Test 1. This change was based on the assumption the electrode coating was the cause of the sticking and allowed determination of the rate of graphite oxidation without such a coating.

- An additional 0.6 m (2 ft) of soil was added above the grade level to provide a total of 1.2 m (4 ft) of overburden above the simulated waste containers. The addition of the overburden was designed to evaluate the effectiveness of overburden in reducing or buffering the effects of the transient gas releases related to vacuum fluctuations.

- An instrumented can identical to that used in Test 1 was installed at the original grade level for an effective burial depth of 0.6 m (2 ft). The can was oriented horizontally (on its side). The can contained 1.8 kg (4 lb) of paper and was instrumented with a pressure transducer and two types of thermocouples. Both thermocouples were inside the can and were located approximately 1 cm from the upper or lower sides. The purpose of the instrumented can was to obtain the temperature and pressure data from the can at the point of gas release and to help define the conditions observed in Test 1.

- The total off-gas flow sensor, the gas sampling port for carbon monoxide and oxygen, and the downstream pressure sensor used to determine the differential pressure for HEPA filter 2 were moved to a point upstream from the blower surge protection inlet. Repositioning the sensor and sampling ports resulted in more accurate measurements due to the surge protection inlet not having a diluting effect.

- Additional instrumentation was added to monitor the incoming three phase power to the transformer to better track imbalances in the transformer. The failed fuses and thyristor switches were on the primary side of the transformer; therefore, the imbalances measured on the secondary side of the transformer were not an adequate measure of the imbalance on the primary side.

- A backup blower was added to the surge pot assembly on the hood so that the magnitude of any hood pressurization would be diminished. The blower was configured to automatically energize itself when the hood pressurized to 1.5 in. of water positive pressure. Although the backup blower could have been configured to energize when the hood vacuum was initially trending toward positive pressure, it was determined that the initial slope of the pressure curve would be best unaltered to allow comparison with Test 1 data.

- Less soil was piled around the base of the hood compared to Test 1. This change was introduced to allow less restriction of off-gas outflow around the base of the hood in the event of a significant hood pressurization as in Test 1. This allowed more air in-leakage during periods of normal operation and resulted in a lower average vacuum in the hood relative to Test 1.

## 4.4 Test 2 Process Data Description

In Test 2 a stacked can layer was placed above the stacked box region and resulted in a notable difference in operations when compared to Test 1. Test 2 was much less dynamic; there were fewer transient conditions in the hood. Electrical imbalances did occur when melting through the stacked can region; however, an improved understanding of this phenomenon, combined with uncoated electrodes, resulted in smoother electrical operations.

Test 2 was initiated at 1540 hours on July 11, 1990. Power to the electrodes was initially brought up to 10 kW, in accordance with the planned graduated power buildup. Over the next 8 hours, power was gradually increased to approximately 400 kW, as shown in Figure 58. Resistance followed the expected curve, peaking at 14 and 13.8 ohms for phases A and B respectively, as shown in Figure 59. This resistance plot shows the gradual transition of

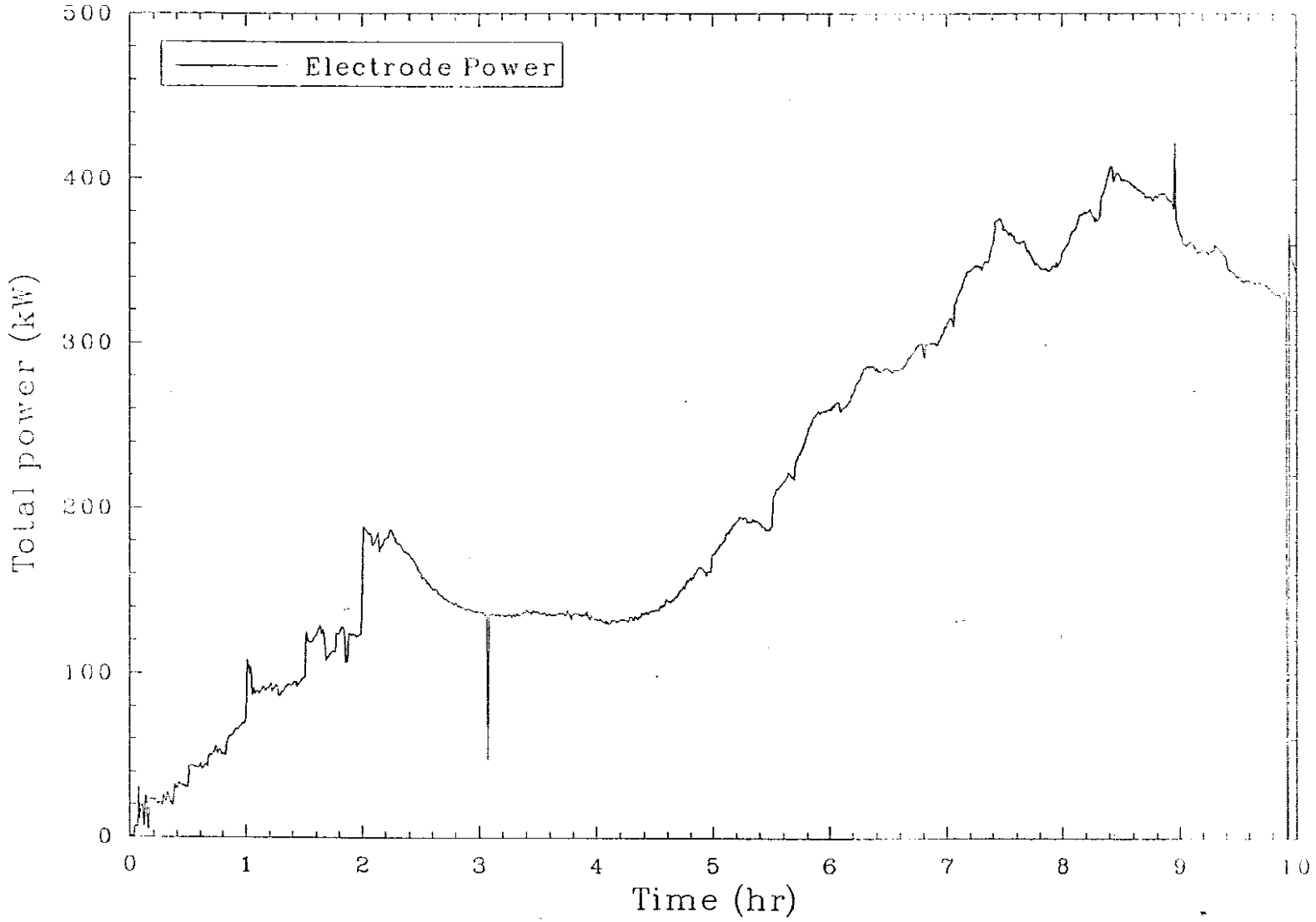


**Figure 58.** Total electrode power showing gradual increase during startup for Test 2.

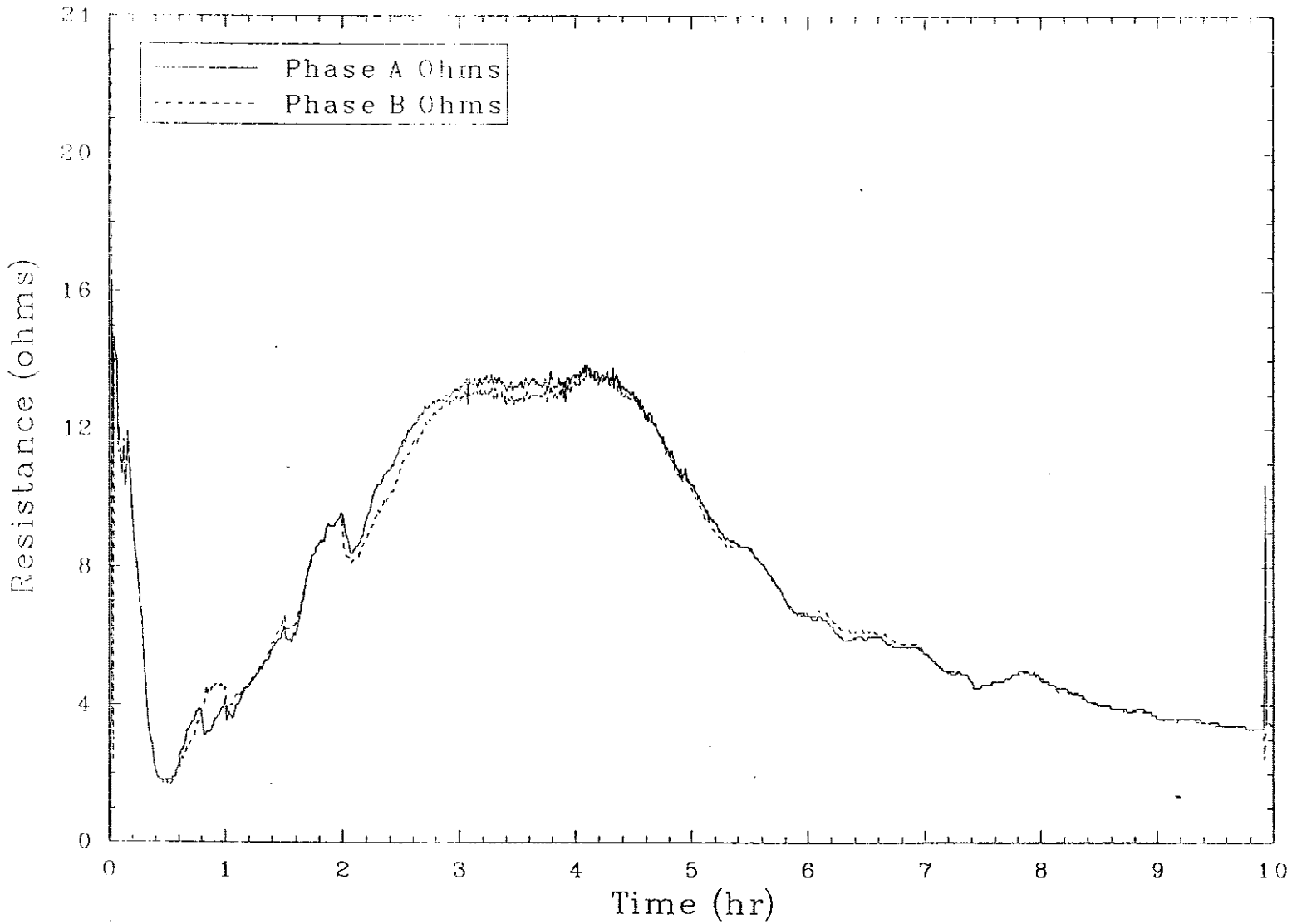


**Figure 59.** Phases A and B resistance during startup for Test 2.

the current path from the starter path to the adjacent molten soil as the path was consumed. At the peak of the resistance, the starter path was totally consumed, and the current pathway existed through the molten soil. The resistance gradually decreased as the molten soil mass increased in depth.

The test duration was 69.5 hours. The total power applied to the melt was 21,300 kWh. The average plenum temperature in the hood was approximately 300°C, although there were two periods of operation above 400°C. The achieved melt depth was 3.9 m (129 in.) as measured in the center of the melt using a steel pipe. The average melt rate was 1.8 in./h. Figure 60 shows melt depth as a function of time. Electrical imbalances encountered in melting through the stacked can region resulted in decreasing the overall melt rate. A summary of the test events is provided in Table 12.

Overall, there were three distinct phases during Test 2 that were well-suited to analyses. Test 2 will be analyzed according to each of the distinct phases, rather than through the analysis of the individual events as was done for Test 1. The three distinct phases involved the following items.

- The instrumented can at the 0.6 m (2 ft) depth
- The layer of stacked cans
- The layer of stacked boxes.

In addition to the analyses of the three test phases, equipment performance including the hood, electrodes, and off-gas treatment system was analyzed in a manner similar to Test 1.

### 4.4.1 Instrumented Can

The instrumented can, identical to that used in Test 1, was installed at the original grade level for an effective burial depth of 0.6 m (2 ft). The can was oriented horizontally (on its side). The can contained 1.8 kg (4 lb)

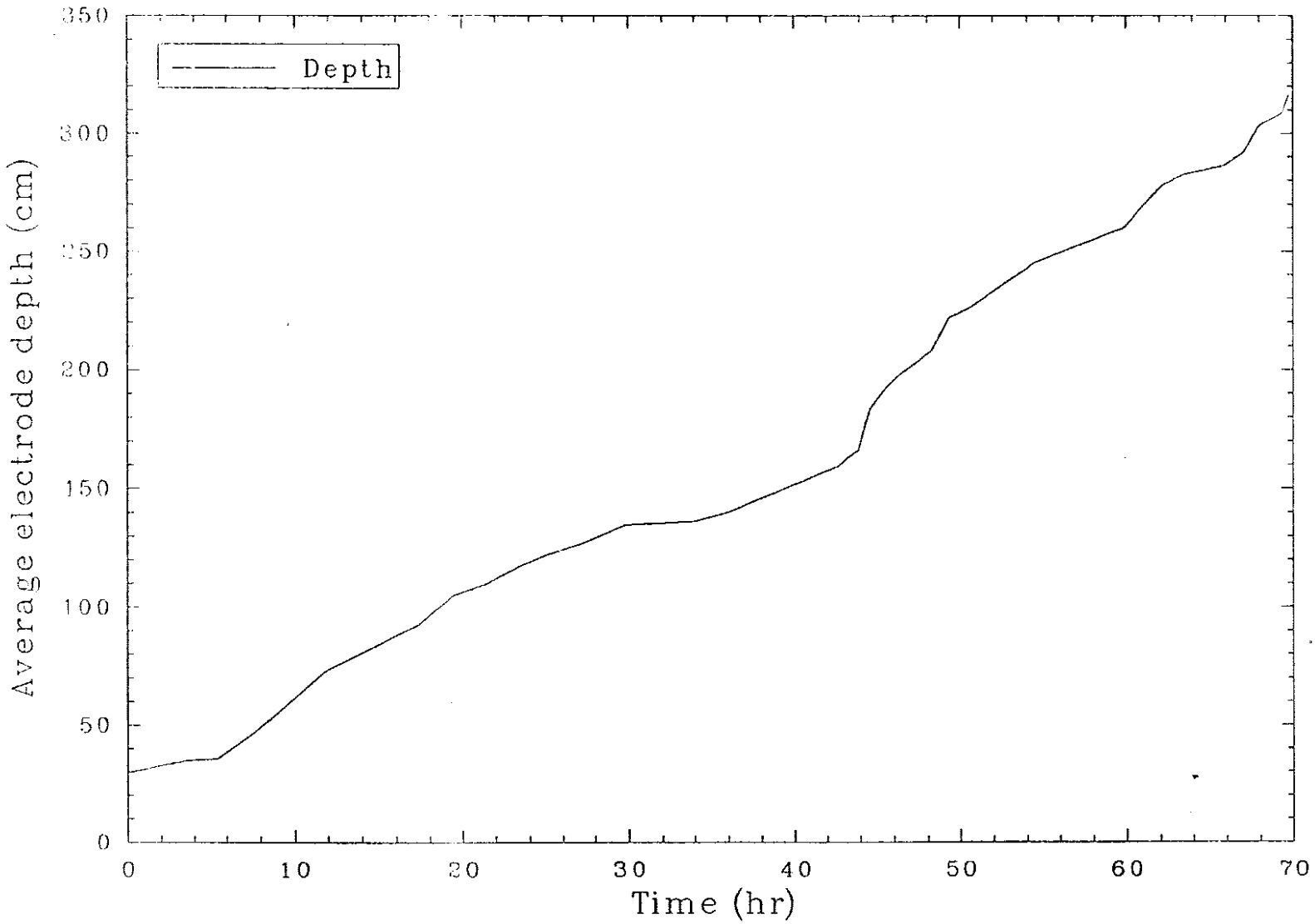


**Figure 60.** Average electrode depth for Test 2.

**Table 12.** Test 2 - summary of events

| Date | Time | Elapsed Time (hour) | Event |
|---|---|---|---|
| 7/11/90 | 1540 | 0.0 | Power to the electrodes. |
| | 1932 | 3.70 | Melt observation indicates entire surface is molten. |
| | 2314 | 7.57 | Melt observation indicates active surface, about 15 cm (6 in.) of subsidence. |
| | 0100 | 9.33 | Average electrode depth 23 in. |
| 7/12/90 | 0150 | 10.16 | Hood pressurization event to approximately 2.9 in. of water. Instrumented can temperatures were less than 100°C prior to event. |
| | 0324 | 11.73 | Average electrode depth 29 in. |
| | 0410 | 12.50 | Several tap changes between the 1000 V and 650 V taps between 0235 and 410 hours. |
| | 0627 | 14.78 | Power temporarily off to fix loose air hose. At ~16 hours can region begins to be thermally influenced by the melt. |
| | 0900 | 17.33 | Average electrode depth 37 in. |
| | 1357 | 24.28 | Power off for 10 min due to transformer thermal trip. Power reduced slightly. |
| | 1655 | 25.25 | Average electrode depth 48 in. |
| | 1749 | 26.15 | Transformer thermal trip. |
| | 1808 | 26.47 | Power restored to electrodes. |
| | 2030 | 28.83 | Hissing sound from within hood. Flare, estimated 91 - 107 cm (36-42 in.), observed. |
| | 2153 | 30.22 | Tap change from 650 V to 430 V. Some fluctuations in amperage subsequently observed. Power was therefore reduced somewhat. |

Table 12. (continued)

| Date | Time | Elapsed Time (hour) | Event |
|---|---|---|---|
| | 2315 | 31.58 | Two saturable core reactor fuses blown. Power off. |
| | 2345 | 32.08 | Power back on. Power is controlled up and down over the next 15-20 min during attempts to establish an electrical balance. |
| 7/13/90 | 0050 | 33.17 | Power balance recovery noted. Phase A = 62.4 kW; phase B = 87.6 kW. |
| | 0140 | 34.00 | Average electrode depth 54 in. |
| | 0150 | 34.17 | Tap change from 650 V to 430 V. |
| | 0345 | 36.08 | Two transformer saturable core reactor fuses blown. |
| | 0705 | 39.42 | Average electrode depth 48 in. |
| | 0840 | 41.00 | Three pops were heard coming from within the hood. Off-gas temperature rises to 300°C. Dust observed rising from around base of hood. |
| | 0945 | 42.08 | A single pop heard from within the hood. Hood pressure increases to +1.9 in. of water and backup blower started momentarily. |
| | 1233 | 44.88 | Breaker trip. |
| | 1240 | 45.00 | Power back on. |
| | 1300 | 45.33 | Melt front at the beginning of the stacked box region. Electrodes average depth is 191 cm (75 in.). |
| | 1540 | 48.00 | Breaker trip. |
| | 1545 | 48.08 | Power back on. |
| | 1700 | 49.33 | Average electrode depth 88 in. |
| | 1900 | 51.33 | Melt observation indicates estimated 1.5 m (5 ft) subsidence. |

Table 12. (continued)

| Date | Time | Elapsed Time (hour) | Event |
|---|---|---|---|
| 7/14/90 | 0552 | 62.2 | All electrodes at approximate equal depth 2.7-2.8 m (9.0 to 9.3 ft): Power balanced. |
| | 0601 | 62.35 | Power off momentarily to drop electrodes. |
| | 1010 | 66.50 | Stack CO observed to be up slightly; assumed due to wooden pallets at bottom of boxes burning. |
| | 1140 | 68.00 | Average electrode depth 120 in. |
| | 1200 | 68.20 | Power off momentarily to drop electrodes. |
| | 1309 | 69.48 | Power off - test completed. |
| | 1552 | 72.20 | Data Acquisition System turned off. |

of paper and was instrumented with a pressure transducer and two Type K thermocouples. Both thermocouples were inside the can and located approximately 1 cm from the upper or lower side surfaces of the can.

At approximately 8.5 hours, the melt started to thermally influence the can. At 8.9 hours, the can reached a maximum pressure of 4.5 psig with the upper thermocouple at 94°C and the lower thermocouple at 88°C (see Figure 61). At approximately 10.2 hours, an apparent gas release from the can caused the hood plenum temperature to spike to approximately 630°C (see Figure 62) and the hood to pressurize to 2.9 in. W.C. (see Figure 63). Immediately after the hood pressurization, an operator noted that the interior surfaces in the hood were covered with what appeared to be soil. A review of the pressure and temperature measurements of the can (see Figure 61) revealed that the can had not depressurized and was maintaining an internal pressure of 4 psig at 94°C for the upper thermocouple. Immediately after the event, the internal can temperature climbed steadily to just over 100°C. Since the can pressure was relatively steady, the temperature increase in the can is suspected to be due

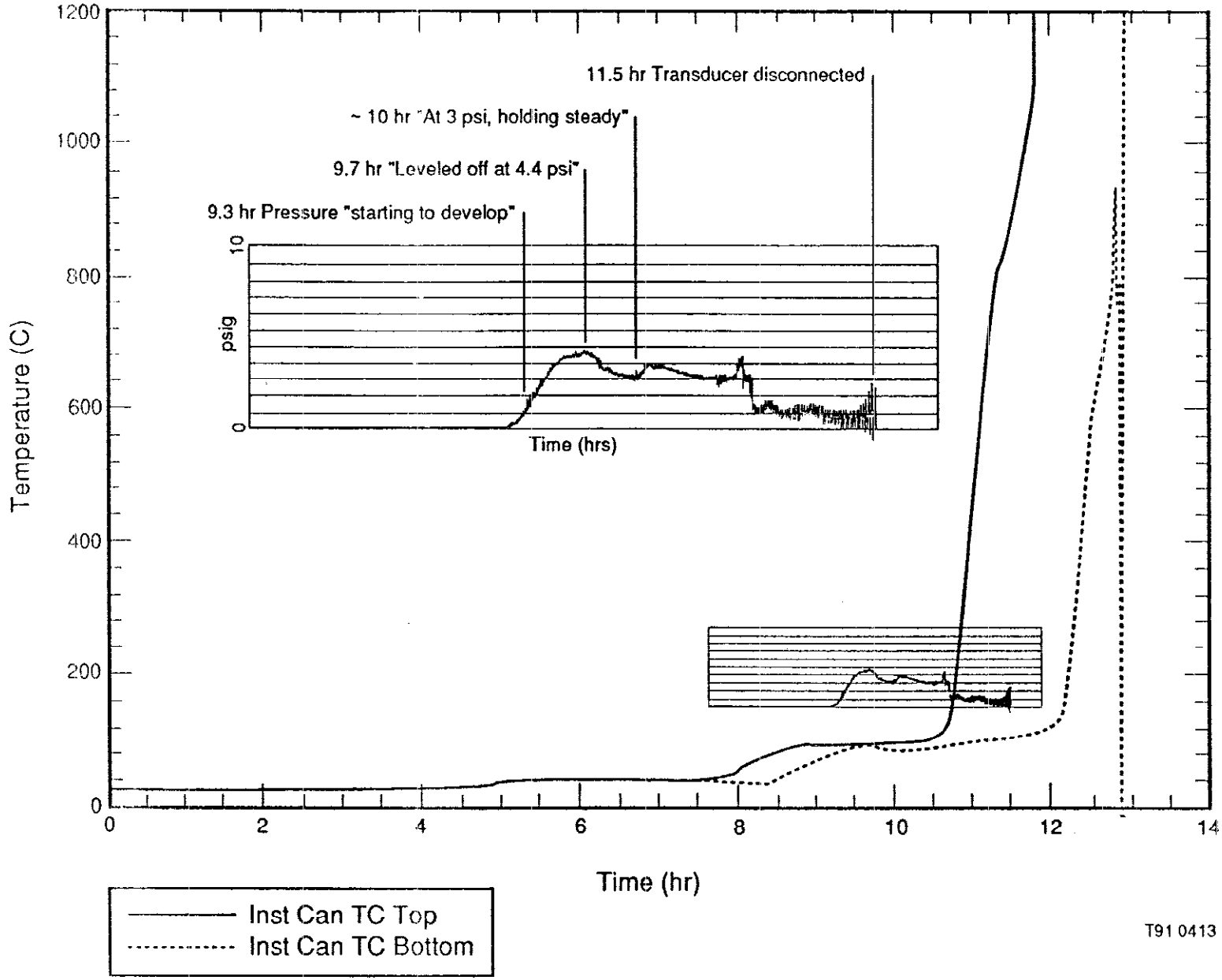


Figure 61. Instrumented can temperatures and can pressure for Test 2.

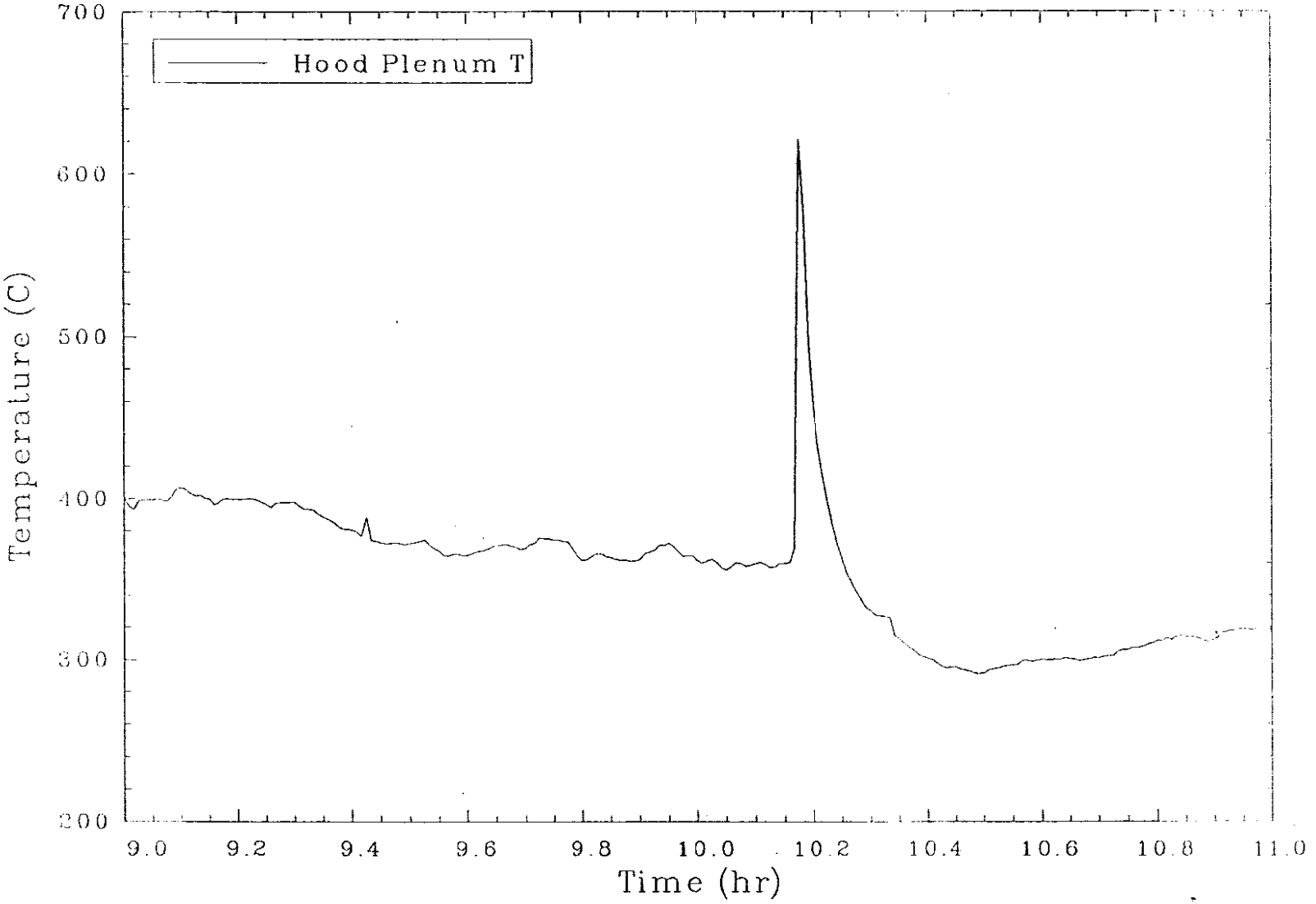


**Figure 62.** Hood plenum temperatures during processing of the instrumented can for Test 2.

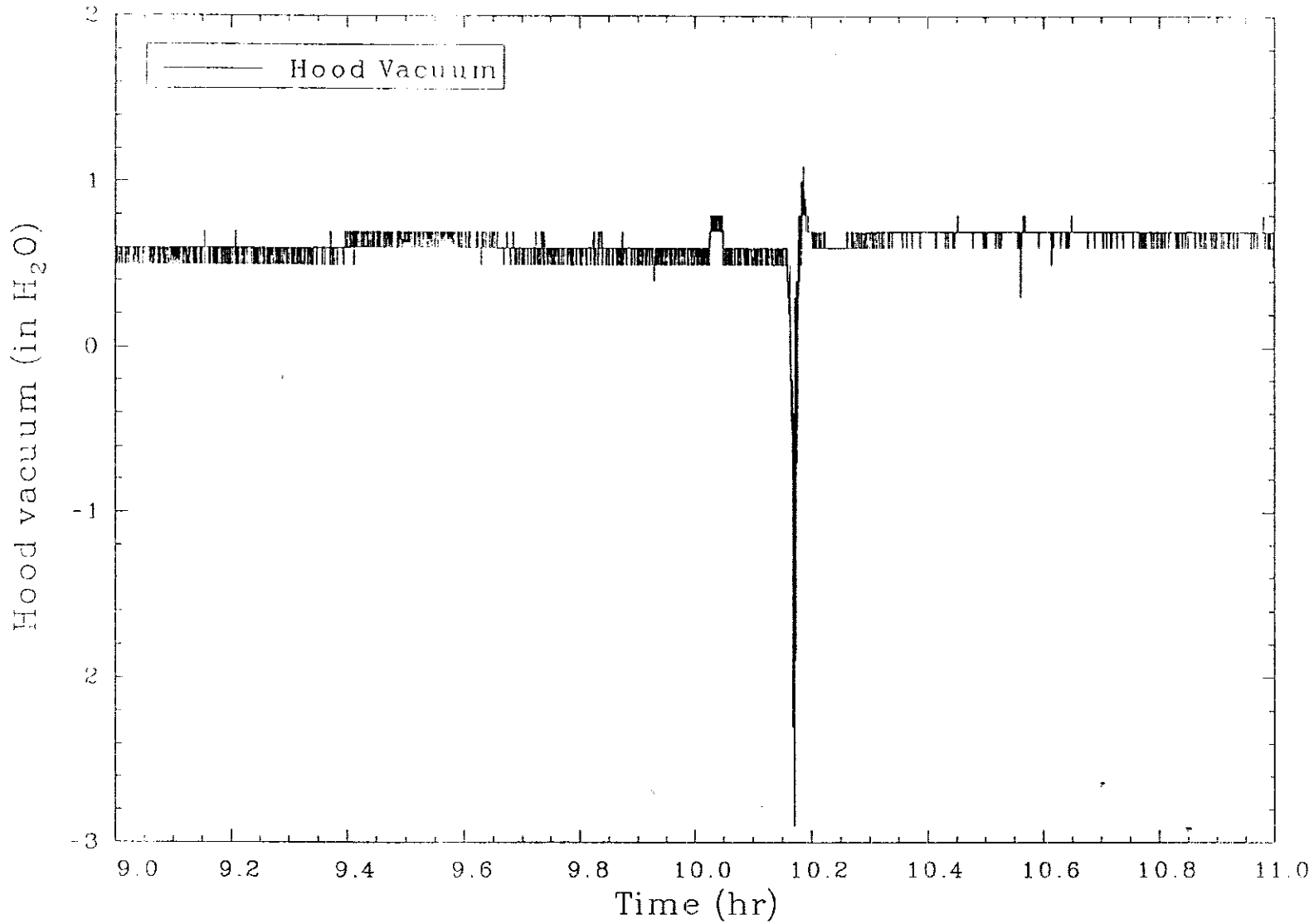


**Figure 63.** Hood vacuum during processing of the instrumented can for Test 2.

to an increased rate of heating of the adjacent soil once the water vapor in the adjacent soil was released.

Since the can did not appear to be responsible for the hood pressurization, the gas release must have been initiated by water vapor from the soil column. It is possible that sudden gas releases can occur from the soil column if the rate of gas or vapor generation exceed the capability of the soil column to dissipate the gas. This condition is dependent upon the gas generation rate (a function of the melt rate and soil moisture), the permeability of the soil column, and the pressure required to release gas through the melt. Gas can release through the melt if the pressure beneath the melt exceeds the sum of the head pressure of the melt and the additional pressure increment required to force gas through the less permeable sintered layer (the incremental zone of soil undergoing the fusing melting process). If pressures are not sufficient to overcome the glass head and to breach the sintered layer, it is likely that the gas will release through the adjacent soil column.

In this event, it is suspected the vapor was released through the melt and, in doing so, entrained a considerable amount of soil. With no heat of combustion, the increased heat measured in the hood must have been due to the addition of superheated water vapor mixing with the gas originally present at nominal conditions with additional radiant heat contribution to the hood shell, thermocouples, and suspended particulate (soil) once the cold cap was disrupted. Since the entire inner surface of the hood and electrodes were covered with soil, it is suspected that extremely heavy loadings of particulate were present in the hood plenum. The temperatures in the hood spiked from 360 to 630°C (270°C increase). The temperature measured at the inlet to the venturi-ejector which would provide a true gas temperature unbiased by thermal radiation inside the hood spiked from 280 to 420°C (140°C increase). A gas release adjacent to the melt would not likely super-heat the gas to this extent; therefore, it is probable that the gas passed through the melt. Additionally, a gas release adjacent to the melt would not likely disrupt the cold cap exposing the significant thermal radiation source of the melt.

Phases A and B resistance values both increased slightly during the event at 10.2 hours, indicating the likelihood that gas had indeed passed through the melt, increasing its electrical resistance. The increased resistance diminished over approximately 12 minutes. The increased resistance was likely due to a cooling action of the melt by the gas, the disruption of the insulating cold cap, and the introduction of some of the entrained soil. Figure 64 shows a plot of A and B phase resistance as a function of time. The total power lost as a result of the event equaled 60 kW.

At approximately 11 hours, the temperatures in the can began to increase dramatically as shown in Figure 61. The can pressure wavered around 4.1 psig before the can suddenly depressurized, causing the hood vacuum to decline from approximately 0.8 to 0.25 in. W.C. At this point, the temperature in the hood increased gradually from approximately 300 to 380°C over a 15 minute period. The internal can temperatures at the time of the release were approximately 510°C for the upper thermocouple and only 98°C for the lower thermocouple. Since the can had a rubber gasket, it is suspected that the release mechanism was a temperature-induced failure of the rubber gasket rather than a structural failure of the metallic sidewall. It is evident that the can was adequately sealed since the pressures in the can were maintained between 4 and 5 psig for several hours prior to the release. If the can was not sealed, it is probable that any water vapor and heated air would have gradually been released over several hours prior to the hood pressurization. The majority of the time the can was at pressure, the temperature in the can was insufficient to produce any other gases, such as decomposition gases, from the pyrolysis of paper.

Later, at 14 hours, the plenum temperature increased again approximately 50°C over a 15 minute period. It is unknown if the can still contained some residual paper that was further pyrolyzed and released at this point since the initial breach of the can occurred 2 hours earlier. Additionally, the collection of pressure data from the can was discontinued shortly after the

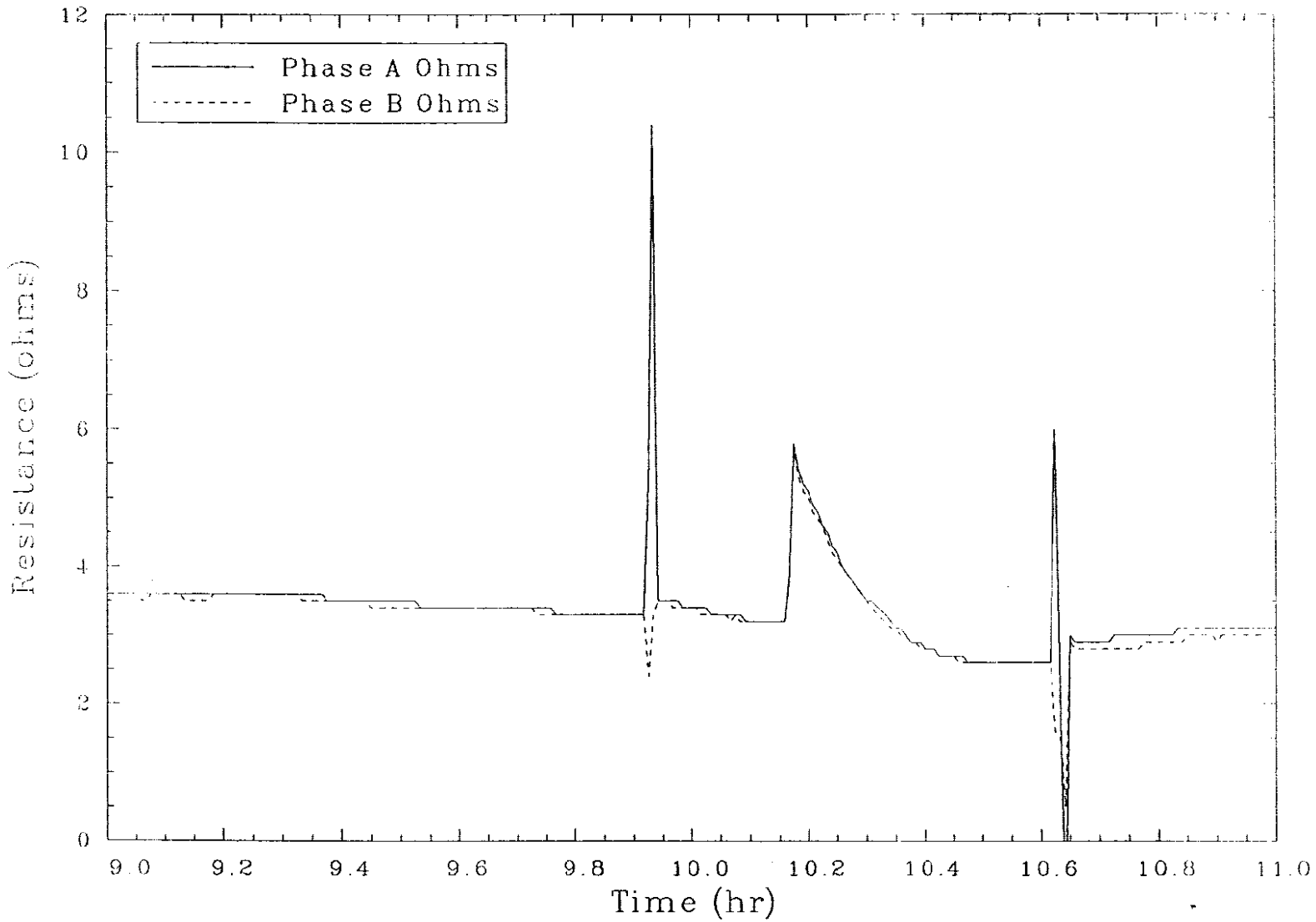


**Figure 64.** Phases A and B resistance during processing of the instrumented can in Test 2.

initial breach since the readings were erratic, indicating transducer failure. It is possible that paper remnants were still present in the can and the can had not fully filled with glass upon initial breach. Previous studies involving sealed containers have shown that glass may flow into cans and temporarily freeze until thermal momentum reetablishes flow to fill the remainder of the can.[8] This explanation would support the increased hood temperatures over the 15 minute period since there were no other known sources of heat generating materials in the vicinity of the melt front. This event did not appear to affect the hood vacuum as the vacuum was relatively steady at 0.8 in. W.C.

It is unknown what created the slight vacuum spike, at 14.5 hours, from 0.8 to 0.25 in. W.C. There was no significant fluctuation in the hood temperature that correlated to the event; however, it is possible that this event was associated with a concluding release from the can.

### 4.4.2 Stacked Can Region

The stacked can region resulted in a slowdown of the downward melting rate and fewer pressure spikes in the hood than experienced in Test 1. The can region appeared to act as a heat sink causing the downward melt progression to slow dramatically, as shown in Figure 65. For approximately 14 hours, the melt front remained at the same depth until all thermocouples in the stacked can region indicated a temperature of at least 100°C. The melt depth, as measured by the depth of the electrode inserted into the melt, did not progress into the can region until the entire can region reached 100°C. A positive consequence of this situation is that most, if not all, water in any of the sludge cans vaporized and escaped from the cans into the surrounding soil well ahead of the approaching melt front. Additionally, the cans released any pressure generated, due to the simple heat expansion of air, well ahead of the approaching melt front. These factors, combined with the additional 0.6 m (2 ft) of soil overburden, effectively prevented the dramatic pressure spikes that were characteristic of Test 1.

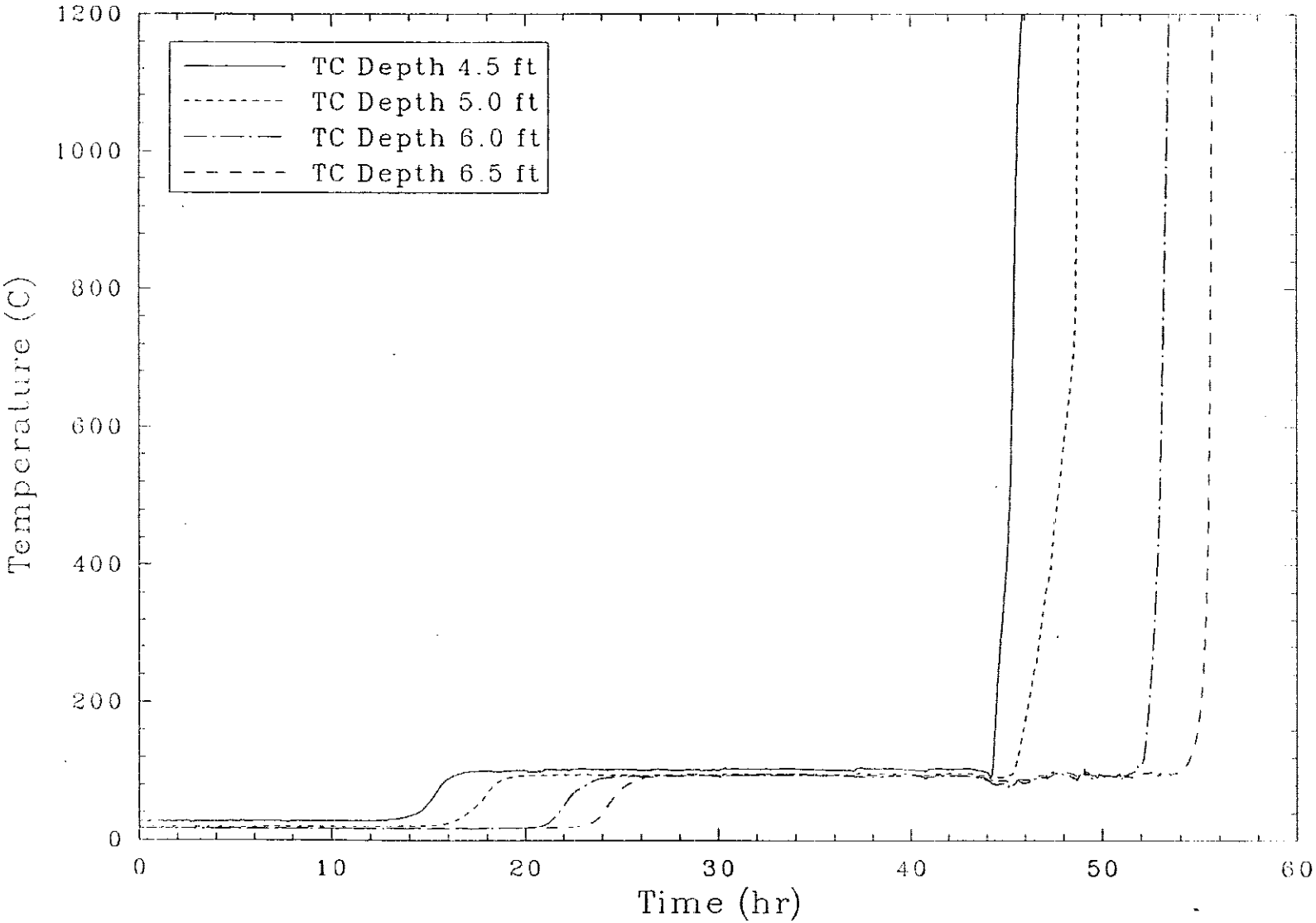


**Figure 65.** Thermocouple temperatures in the stacked can region for Test 2.

As the melt progressed into the can region, power imbalances hampered operations of the transformer. The positive aspect of the situation was that the electrodes were free to be adjusted to compensate and control the electrical imbalances. At several points during the processing of this region, electrode power was significantly reduced or turned off during attempts to adjust the position of the electrodes and to regain a power balance between phases A and B. Based on current large-scale transformer designs utilizing independent secondary control, the imbalances could have been more effectively controlled with secondary control and adjustment of the electrode positions. Because it has a single controller for both secondary phases, the intermediate-scale system design limits the operator's control options to electrode movement. Figure 66 illustrates the power disruptions associated with this region. From approximately 20 to 40 hours, total power levels averaged less than 200 kW as compared to an overall test average of 300 kW. Figures 67 and 68 illustrate the imbalances between the secondary phases, with Figure 67 plotting phases A and B voltage and Figure 68 plotting amperes for both phases. At 31.5 hours and again at 32 hours into the test, the most significant imbalances measured on the primary side of the transformer were observed. These are listed in Table 13. A general operating guideline is to maintain balance on the primary side within 20%. At greater imbalances for periods exceeding 20 to 30 minutes, the saturable core reactor fuses tend to fail due to excessive heat. This type of fuse failure is precisely what occurred at 31.6 hours. Two of six saturable core reactor fuses failed due to the 25 to 33% (100 A) imbalance in the transformer. A large-scale transformer designed with independent control of the secondary phases would be capable of accommodating these imbalances without significant difficulty.

There are several causes for the imbalances.

- As the melt contacted and melted through the can region, cans randomly failed and were filled with glass. This continuing process resulted in the bottom surface of the melt to be irregularly shaped, resulting in partially melted containers that disrupted the current pathway between the opposing electrodes.

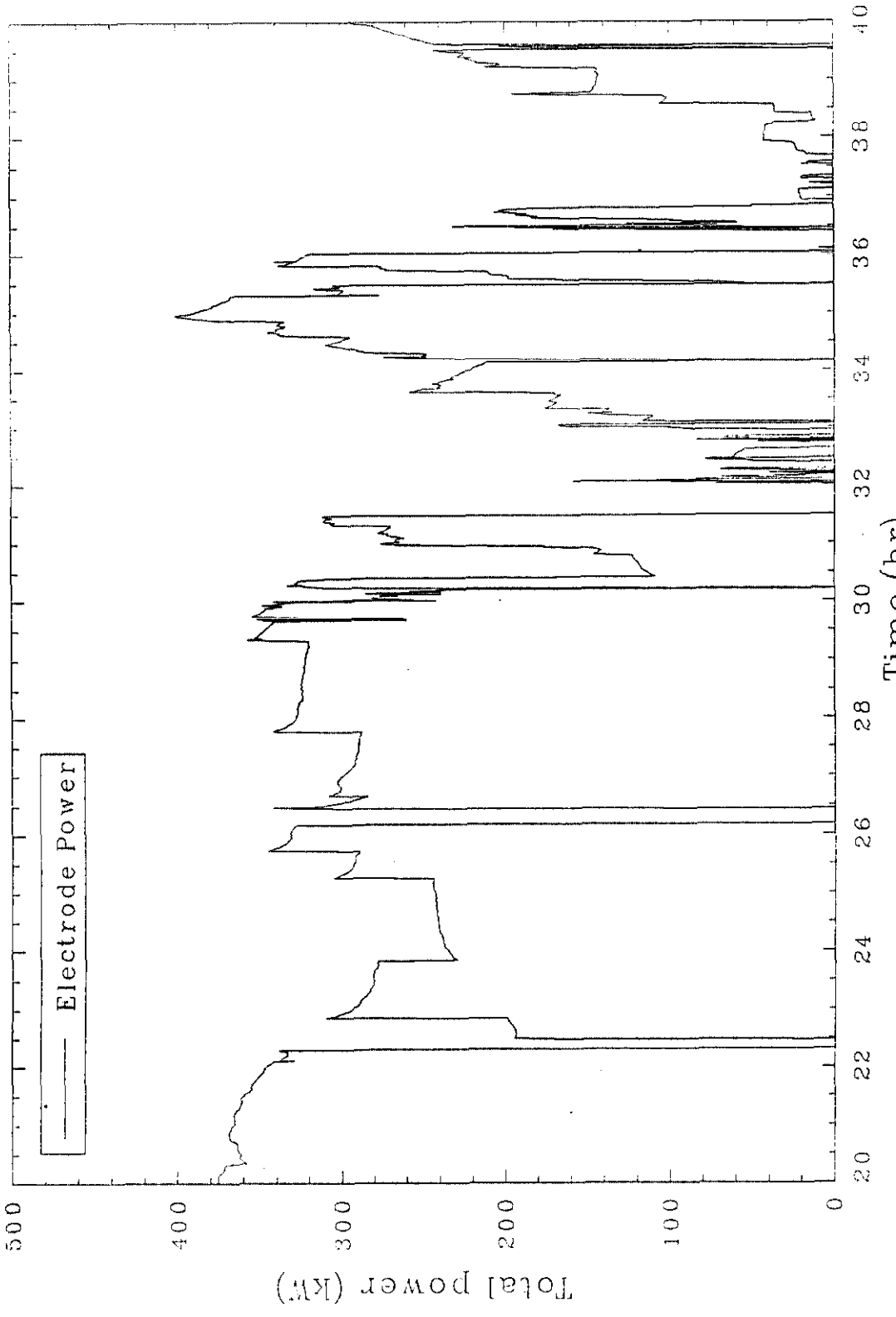


Figure 66. Total electrode power during processing of the stacked can region on Test 2.

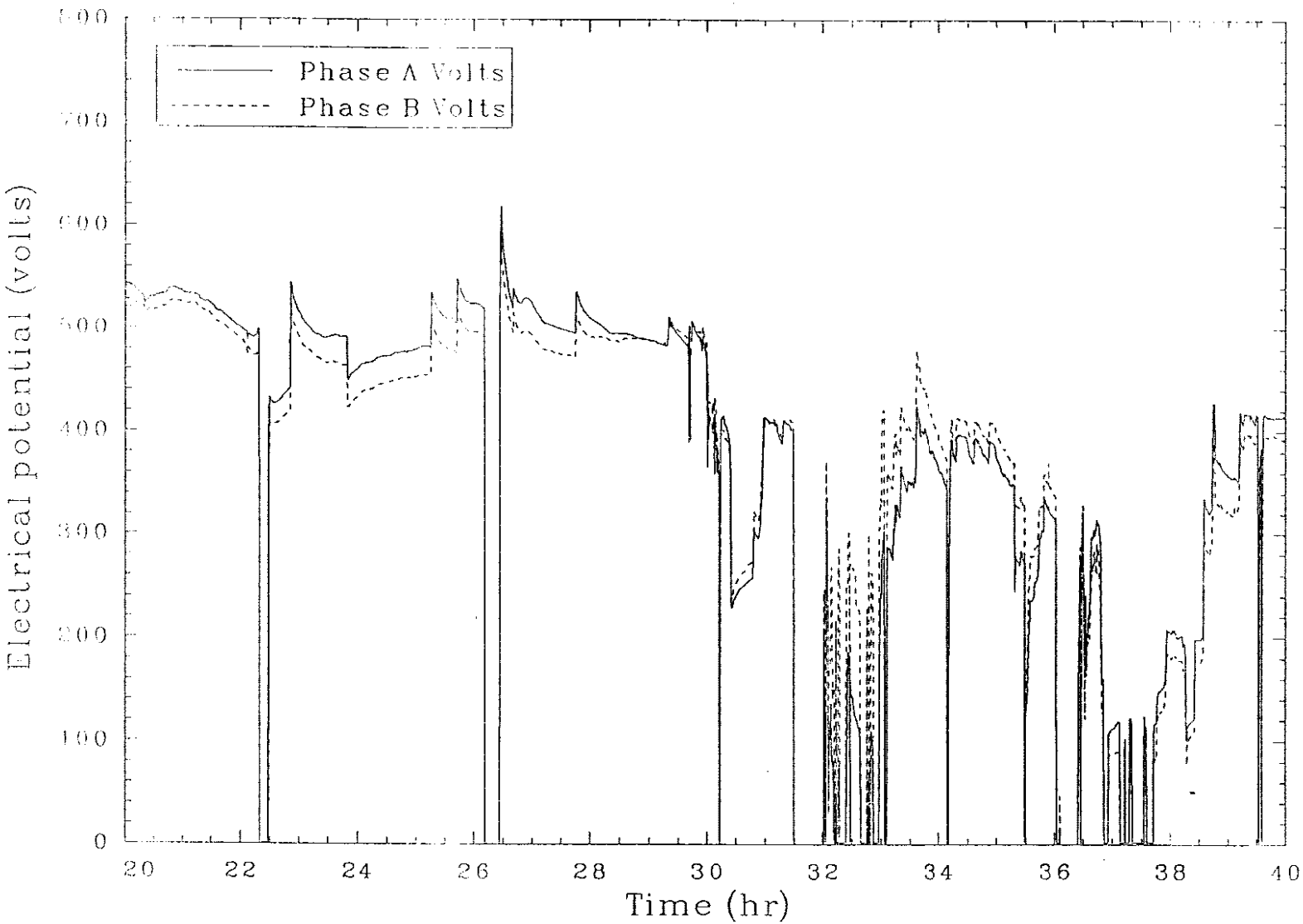


**Figure 67.** Phases A and B voltage during processing of the stacked can region for Test 2.

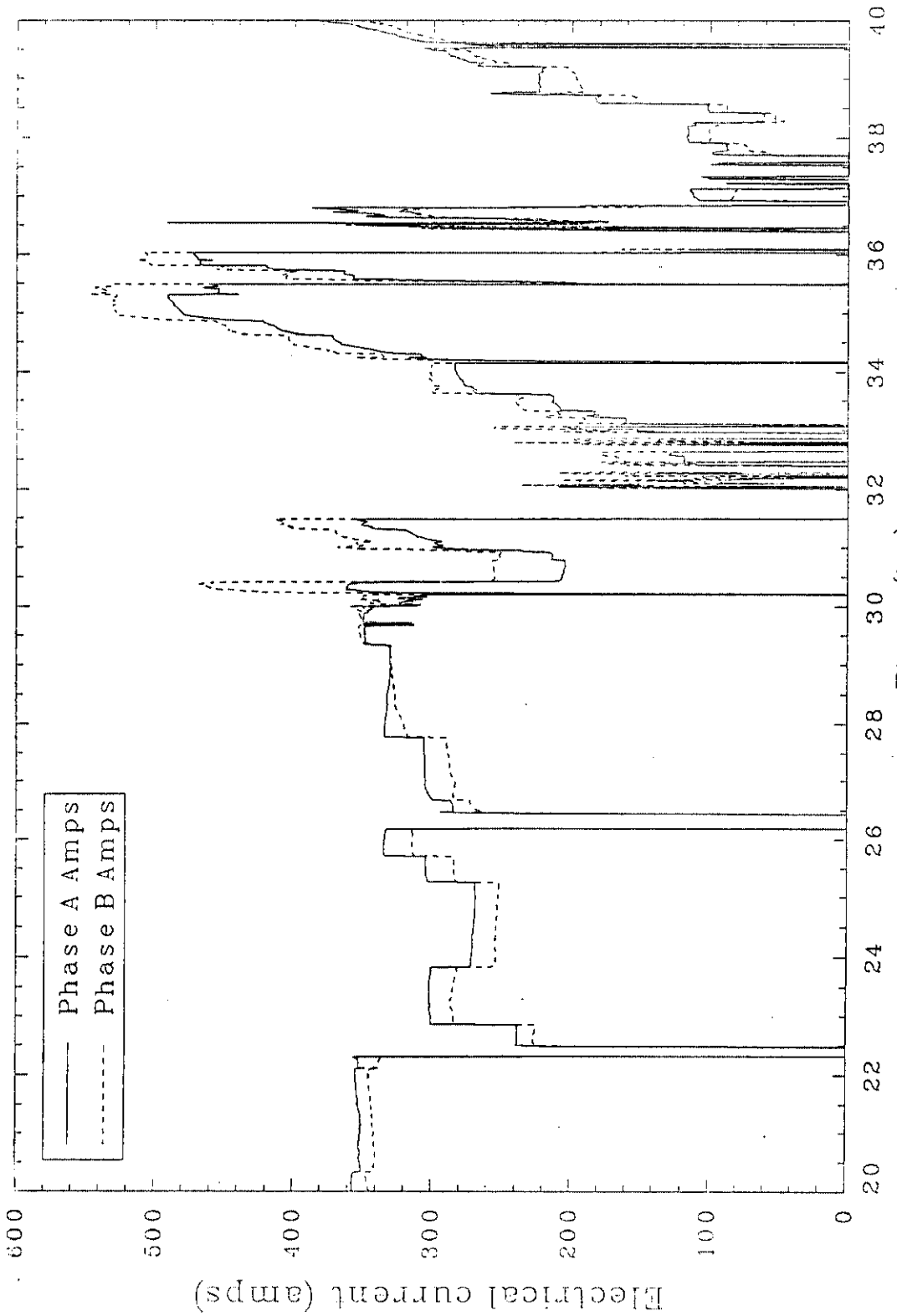


Figure 68. Phases A and B amperage during processing of the stacked can region for Test 2.

Table 13. Primary amperage

| Run Time (hours) | A Phase | B Phase | C Phase |
|---|---|---|---|
| 31.5 | 285 | 196 | 291 |
| 32.0 | 385 | 295 | 392 |

- As a result of Test 1 operations and the fact that Test 2 contained a higher percentage of metal, new electrode control measures were implemented. To help eliminate the possibility of encountering a direct electrical short of two opposing electrodes contacting a single molten metal pool, opposing electrodes were slightly staggered relative to the insertion depth. This operating philosophy resulted in some imbalance because the primary firing pattern between opposing electrodes was partially disrupted, creating an unequal electrode surface area available in the melt for conduction. Because imbalances were occurring, operational modifications were made to equally insert electrodes.

- After operational modifications, some imbalances persisted. Electrodes resting on the bottom surface of the melt in the can region contacted metal cans and created a highly conductive current pathway through the upper layer of partially melted cans to the opposing electrodes. Therefore, an additional operational modification was made to grip and hold the electrodes a few centimeters above the bottom surfaces of the melt, above any molten metal. This change resulted in a more balanced electrical operation.

The total glass depth at the time of the imbalances was less than 0.6 m (2 ft) based on a final glass depth of less than 1.2 m (4 ft) at the conclusion of the test. This minimal glass depth tends to exaggerate the consequences of an imbalanced situation. Once all electrodes were retracted to an equal insertion depth of several centimeters above the bottom of the melt surface and after inclusions contributing to the initial imbalanced situation finally melted to create a relatively unrestricted, electrically conductive pathway

through the molten glass, a balance between the phase A and B power input was achieved and maintained at approximately 50 hours.

The only notable gas releases from cans in the region occurred at 30.0, 41.1, 41.8, and 42.1 hours. An operator observed at approximately 30 hours flares estimated to be 1 m (3.3 ft) in height. At that point during the test, the plenum temperature data revealed a minor rise of approximately 15°C. Hood vacuum was essentially unchanged at 0.9 in. of water. This data is provided in Figure 69. The carbon monoxide concentration at 30 hours was stable at 0.1% and did not indicate any increase. No changes in electrical power or resistance were observed at that specific time during the test. The second gas release, at approximately 41.1 hours, was audible and was described by operators as a series of three pops emanating from the hood at approximate 1 second intervals. Hood vacuum fluctuated from 0.8 in. of water vacuum to 4.0 in. of water pressure over a 16 second period, then spiked 6 seconds later from 0.75 to 0.1 in. of water vacuum. The hood plenum temperature spiked from 230 to 295°C. The third event occurred at 42.1 hours. In the third event, hood vacuum spiked from 0.75 in. of water vacuum to 2.25 in. of water positive pressure over a 29 second period. The hood plenum temperature increased from 240 to 340°C. This series of events is depicted in Figure 70.

Because the gas releases at 41.1 hours were accompanied by three audible "pops", it follows that the gas was released from containers at or slightly above the glass surface along a side wall because the molten glass would tend to muffle the sound of any release. In addition, the magnitude of the pressure spikes were greatly diminished in Test 2 relative to Test 1 primarily because of the additional glass volume created by increased soil overburden. Because the first gas release lasted over 16 seconds, it is likely the last two of the three audible gas releases at 41.1 hours occurred during the initial 16 second period.

Phase A and B resistance did not fluctuate during this series of events, as shown in Figure 71. The spikes shown at 42.6 hours in this figure are not

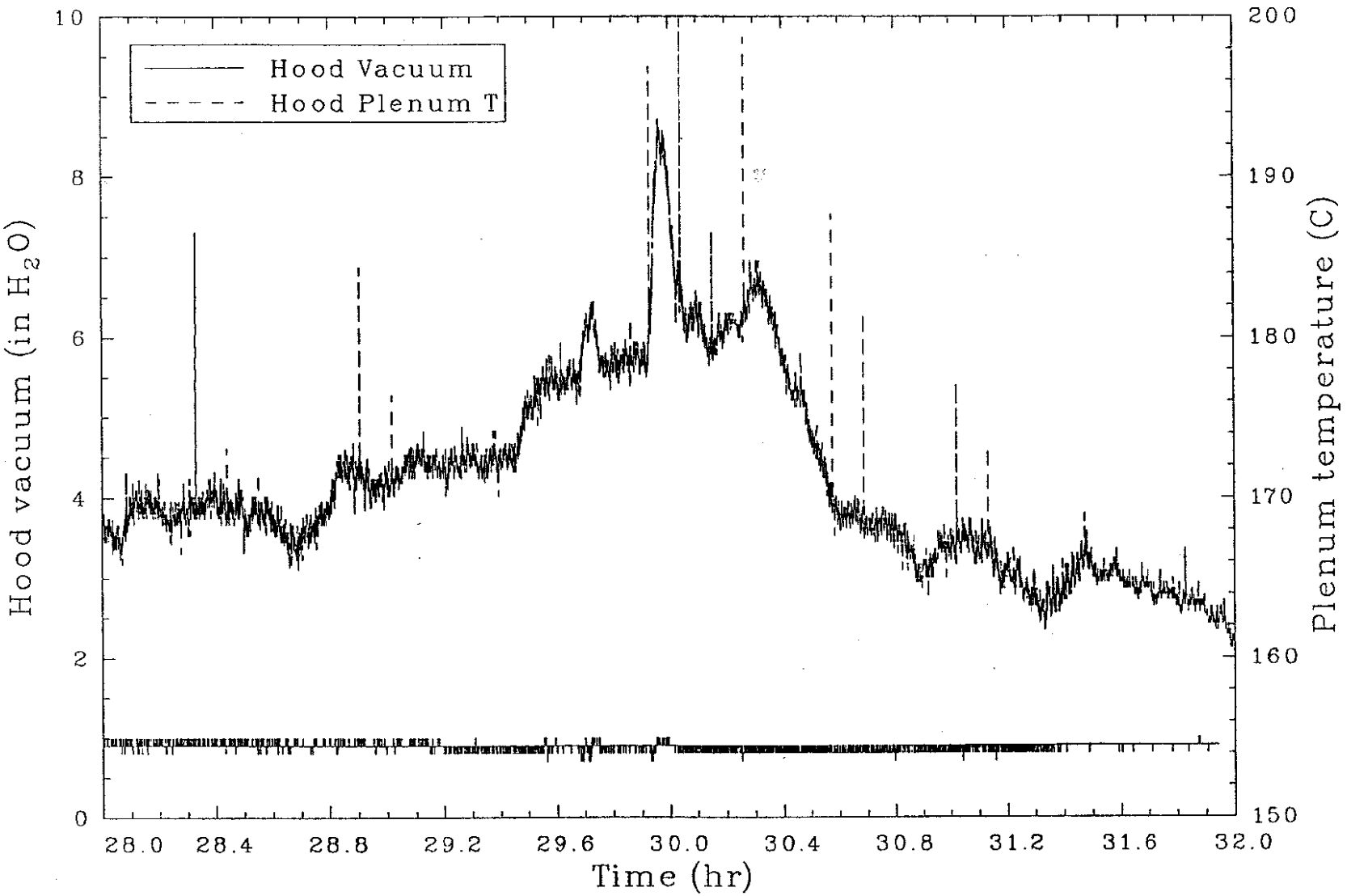


**Figure 69. Hood plenum temperature and hood vacuum at approximately 30 hours, Test 2.**

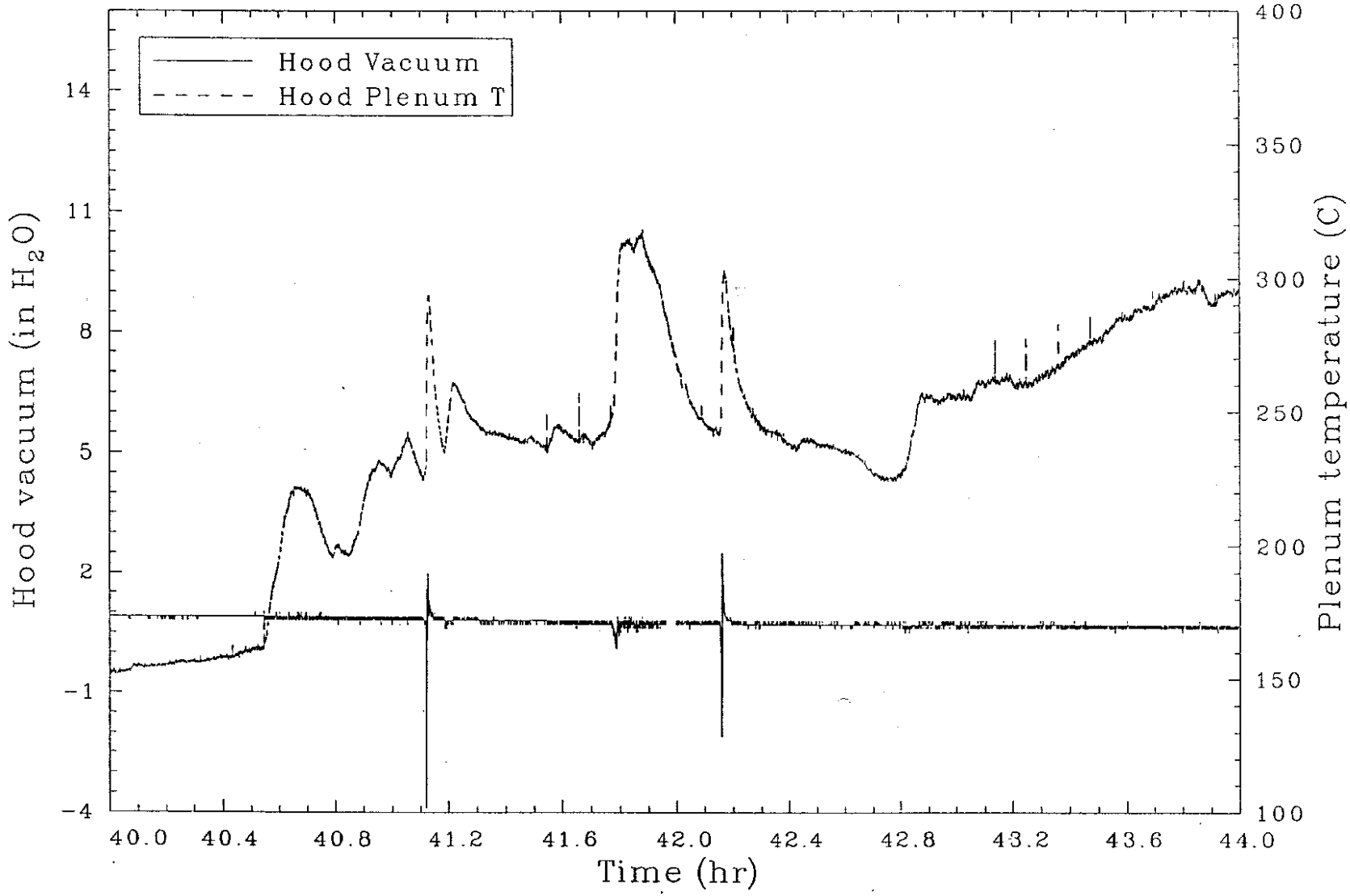


**Figure 70.** Hood plenum temperature and hood vacuum for several gas release events during processing of the stacked can region in Test 2.

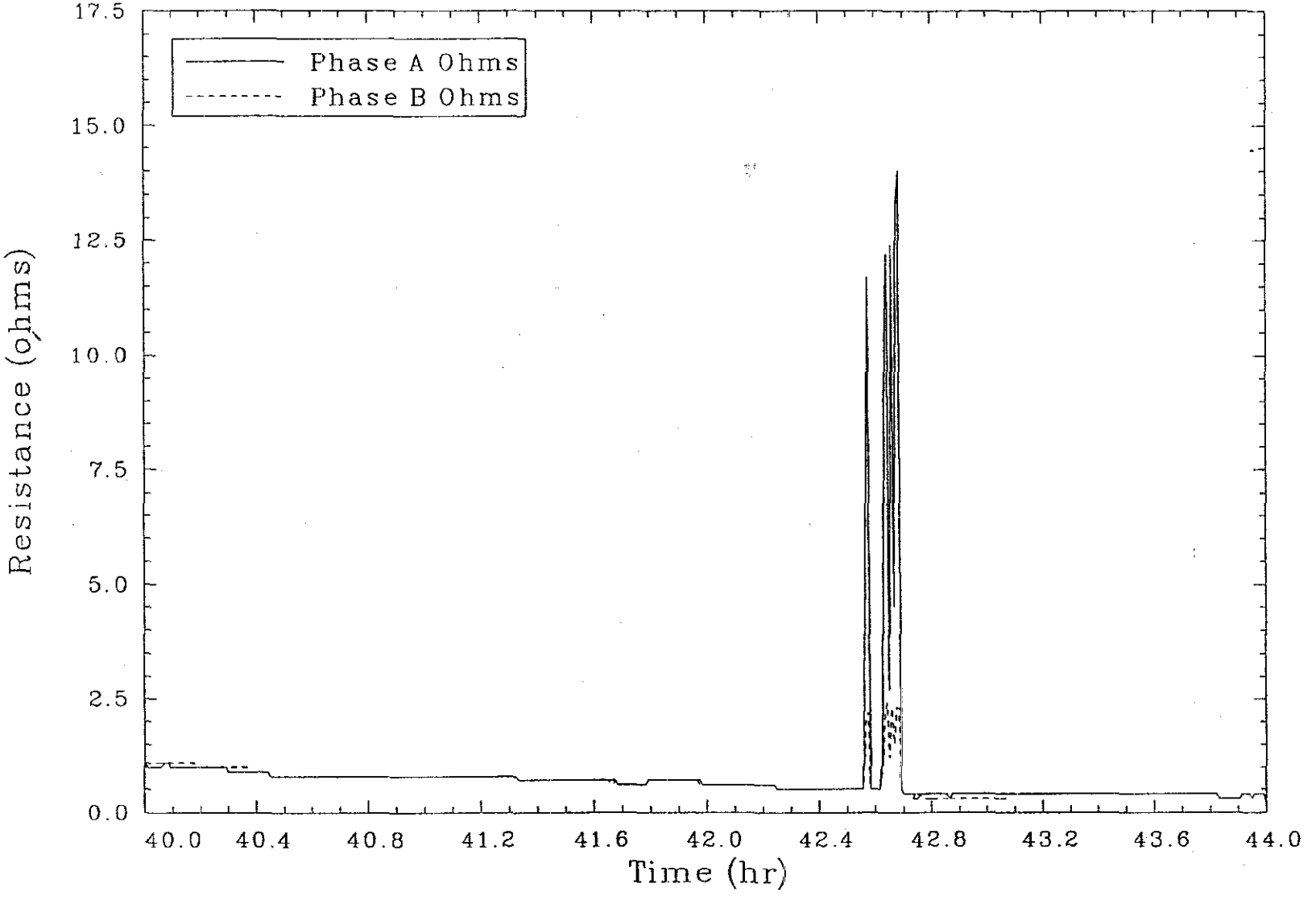


**Figure 71.** Phases A and B resistance for several gas release events during processing of the stacked can region in Test 2.

correlated with the gas releases. Total power levels, as well as amperage or voltage, did not fluctuate to any significant degree due to the gas releases. This indicates the gas releases were not complicated by disruptive inclusions in the melt or by other mechanisms such as melt cooling, which would increase the resistance of the melt and decrease the power input levels.

### 4.4.3 Stacked Box Region

The stacked box region, consisting of high metal content waste intermixed with soil, resulted in an entirely different operational behavior compared to the stacked can region. The stacked box region was encountered at approximately 1300 hours on July 13 at a run time of approximately 45 hours. At the time the stacked box layer was encountered, hood plenum temperatures had increased to 300°C, following the imbalanced period of operation between 30 and 40 hours, as shown in Figure 72. Since approximately 40 hours run time, the hood vacuum had been declining gradually and at 40 hours had reached a relatively steady state level of 0.5 in. of water, from an original level of 1.9 in. of water. This decrease in vacuum is due to an increased generation rate of off-gas from the melt. The hood plenum temperature spiked from 360 up to 490°C at 48 hours and again from 400 up to 440°C, as shown in Figure 73. In each case, increased temperatures did not immediately decline as in previous temperature spikes but remained elevated at the peak values for several minutes. These temperatures represented the highest sustained temperatures observed during the test and are due to extensive and continued pyrolysis and combustion of the top layer of boxes. Due to the extensive combustion occurring in the hood, the hood vacuum spiked downward at this same point during the test--from an initial level of 1.0 down to 0.1 in. of water vacuum. The vacuum level decreased, but, unlike previous vacuum spikes, this event had more of a gradual downward trend and was sustained at 0.1 in. of water for several minutes, as shown in Figure 74. There is a gap in data at approximately 47 hours; however, the second pressure transducer indicated a gradual decrease of vacuum to the 0.1 in. of water during that time period.

During the processing of the stacked box region, power levels averaged 300 to 350 kW, as shown in Figure 75. The high metal content of this region

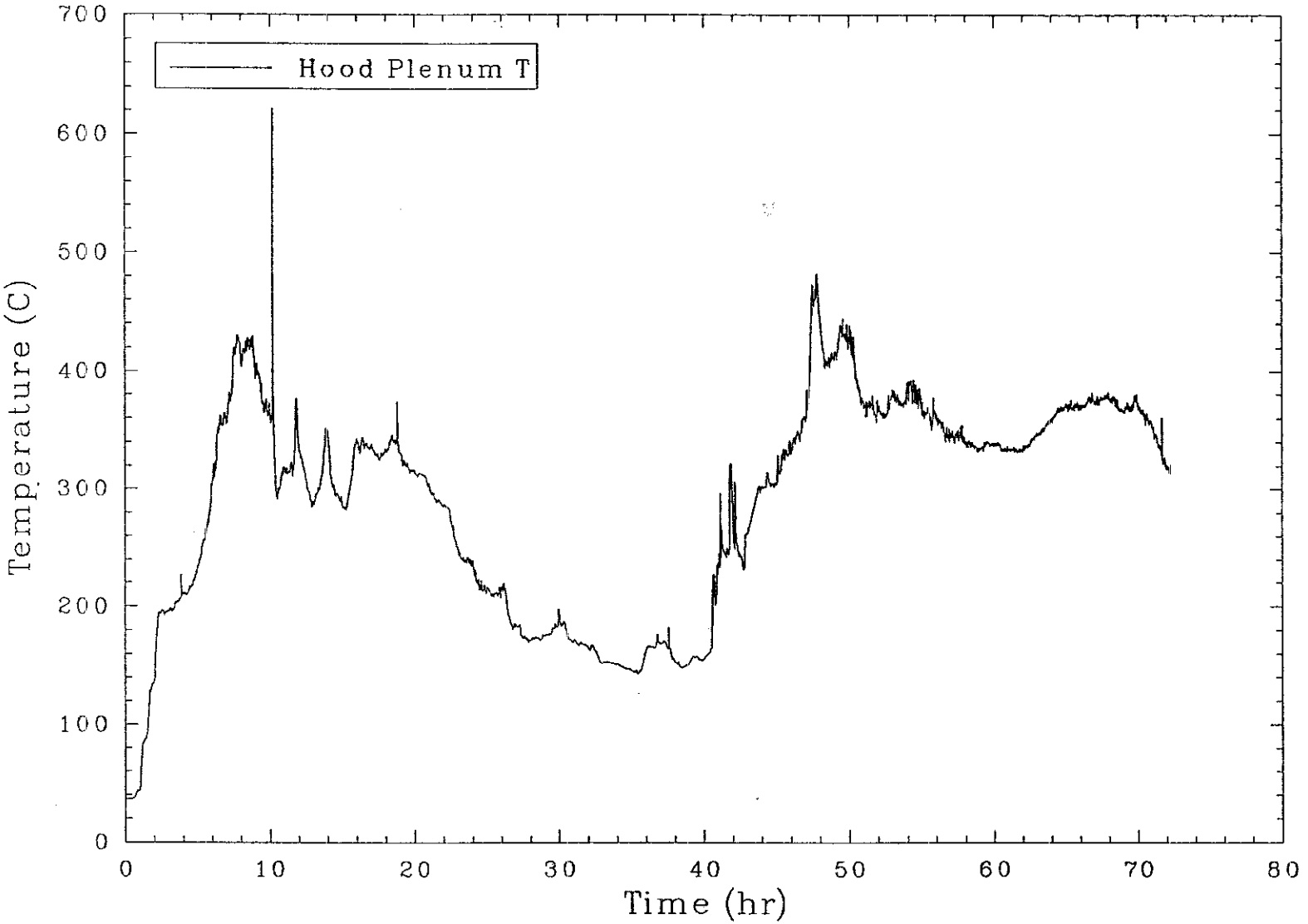


**Figure 72.** Hood plenum temperatures showing gradual increase prior to encountering the stacked box region in Test 2.

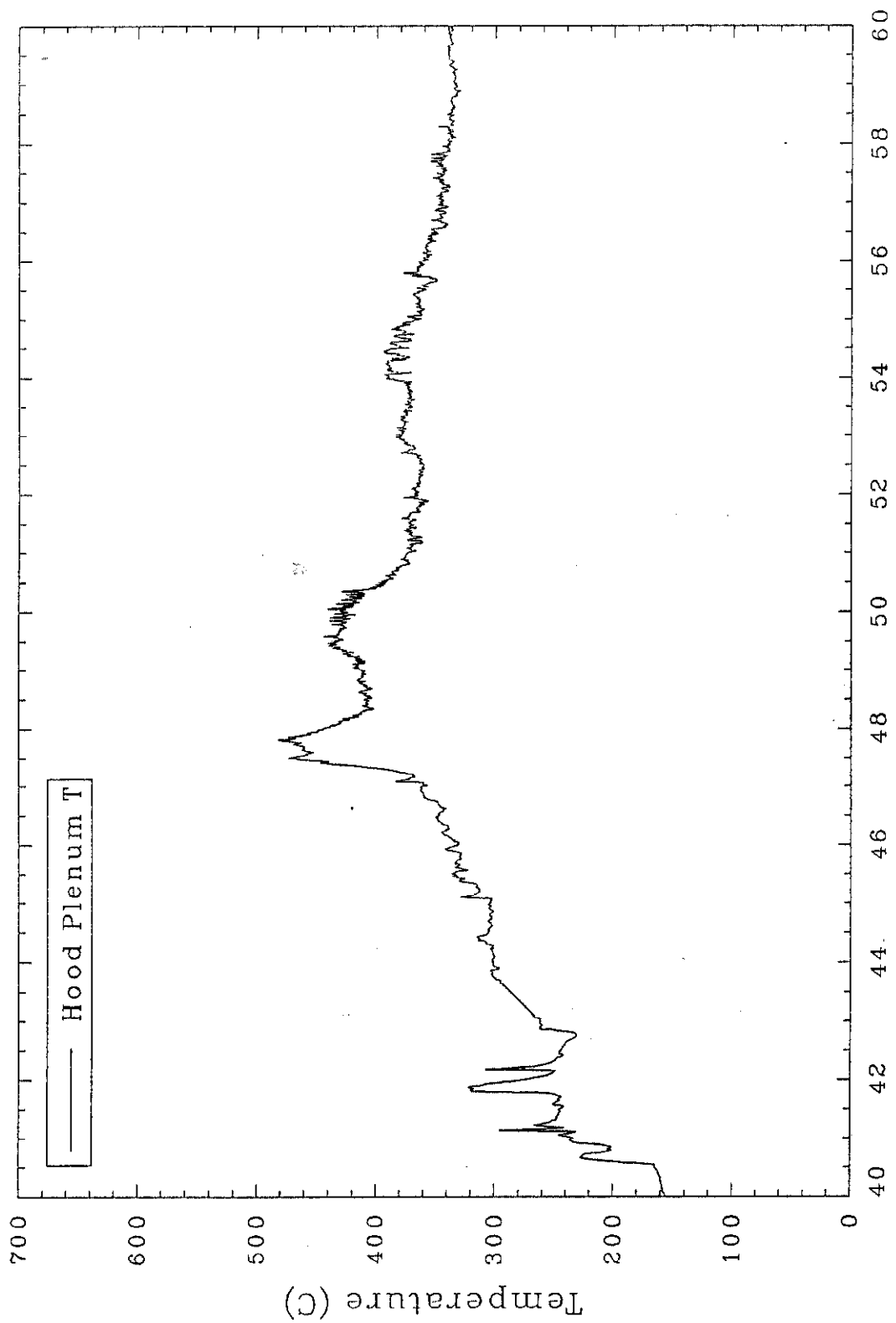


**Figure 73.** Hood plenum temperature showing temperature increases at 48 to 50 hours during processing of stacked box region, Test 2.

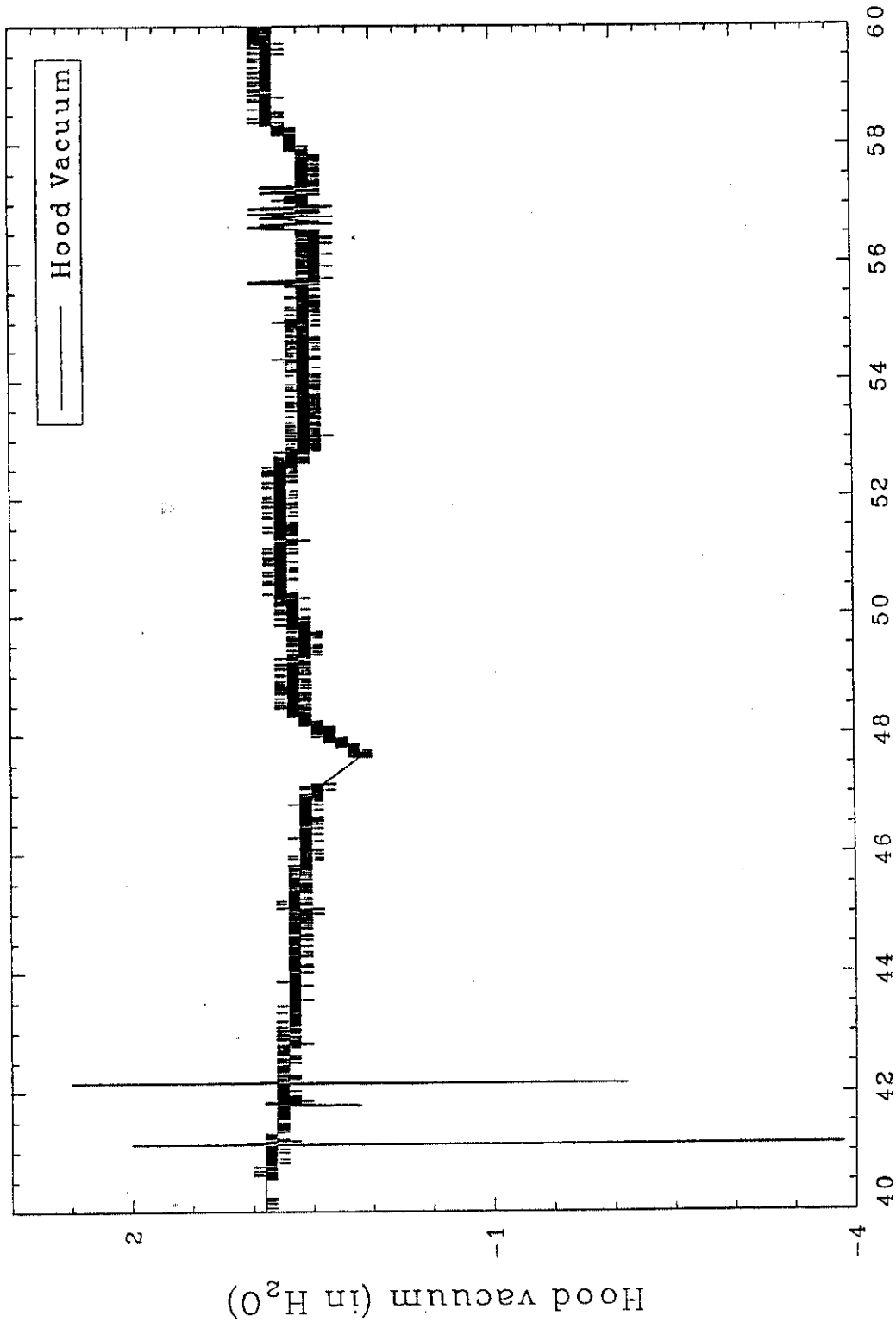


**Figure 74.** Hood vacuum showing mild decrease during processing of the top layer of stacked boxes for Test 2.

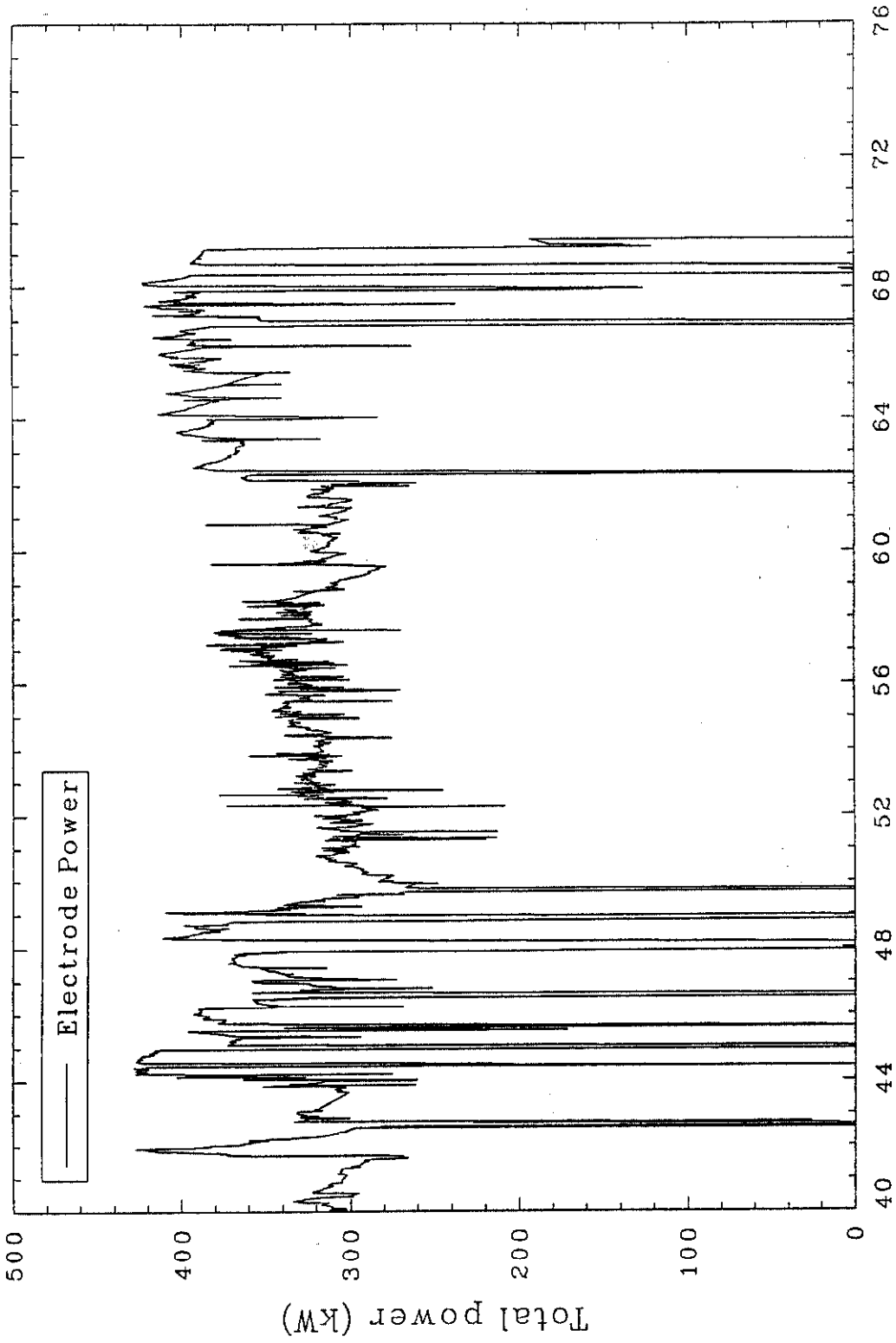


**Figure 75. Total electrode power during processing of the stacked box region for Test 2.**

combined with the molten metal from the stacked can region did not hamper electrical operations of the transformer. The reasons for the smooth electrical operations relative to Test 1 include (a) the electrodes were free, allowing their insertion depths to be adjusted as needed, (b) the electrodes were continually suspended above the molten metal at the bottom of the melt, and (c) the mass of the melt was increased relative to Test 1 due to increased overburden. No significant fluctuations in resistance were observed, and resistance averaged less than 1 ohm for both phases. From 48 hours through the remainder of the test, voltage consistently averaged 220 for both phases A and B.

Both secondary phases averaged 800 A over the final 22 hours of the test, as shown in Figure 76. At approximately 68 hours, power to the electrodes were deenergized and the electrodes allowed to rest on the bottom surface of the melt to confirm the depth of the melt. Melt depth was confirmed at an average electrode depth of 3.1 m (122 in.).

### 4.4.4 Equipment Performance for Test 2

The off-gas hood performed exceptionally well during Test 2. The temperatures observed in the hood represented the highest sustained temperatures ever recorded in the hood. No thermal degradation of the hood, RTV-106 sealant, or electrode seals resulted from the test.

Like Test 1, the off-gas treatment system performed well with respect to cooling the off-gas stream. This is illustrated by Figure 77, which provides the inlet and exit temperatures of the Venturi-Ejector and shows that the heat was effectively removed from the off-gas stream by the Venturi-Ejector.

The off-gas treatment system effectively removed particulate from the off-gas stream. Figure 78 illustrates that the efficient scrubbing action did not result in a gradual plugging of the filters due to particulate buildup. The sudden decrease in pressure at 48 hours reflected the increased rate of off-gassing from the melt and the corresponding decrease in hood vacuum. The

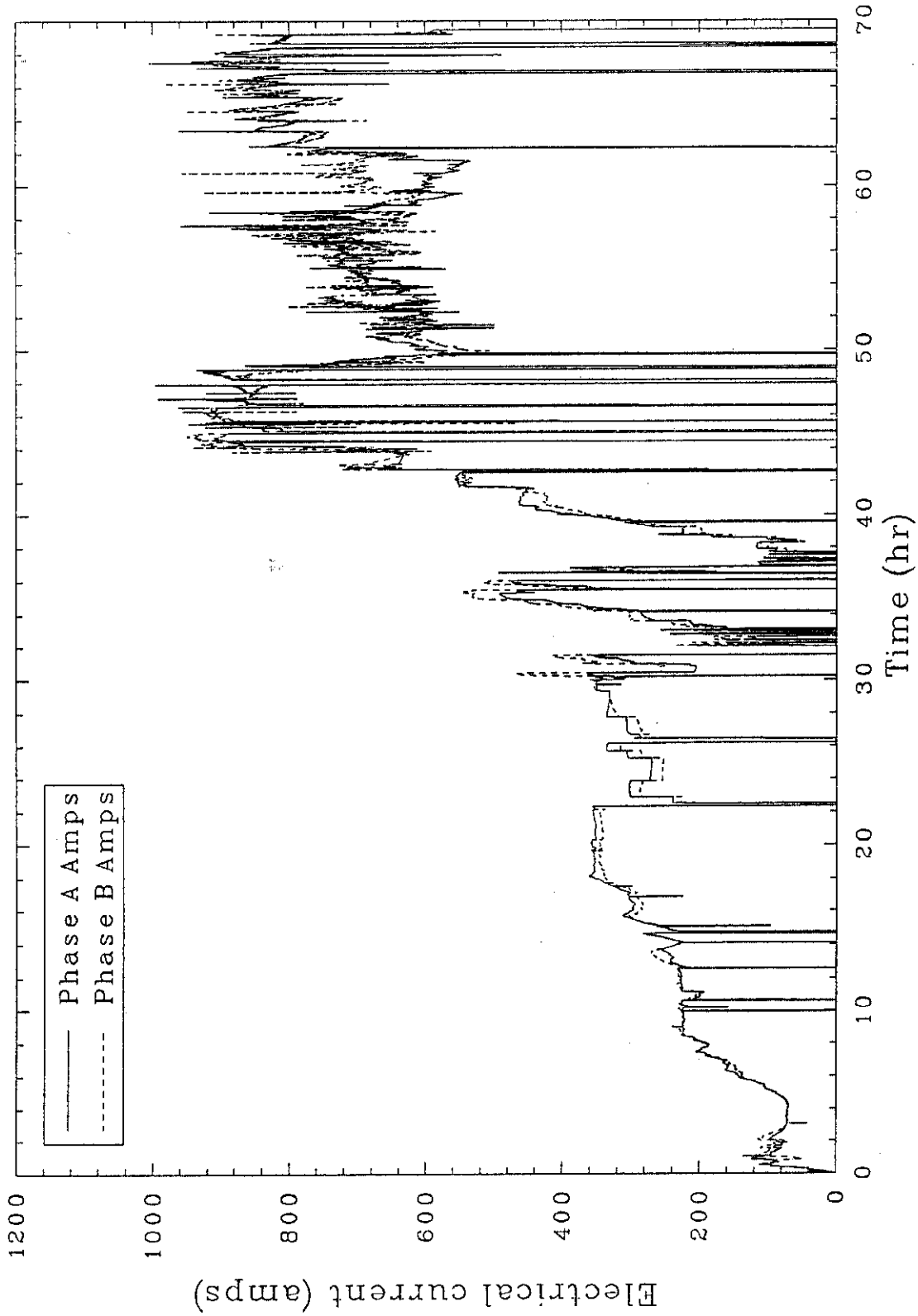


**Figure 76. Phase A and B amperage for Test 2.**

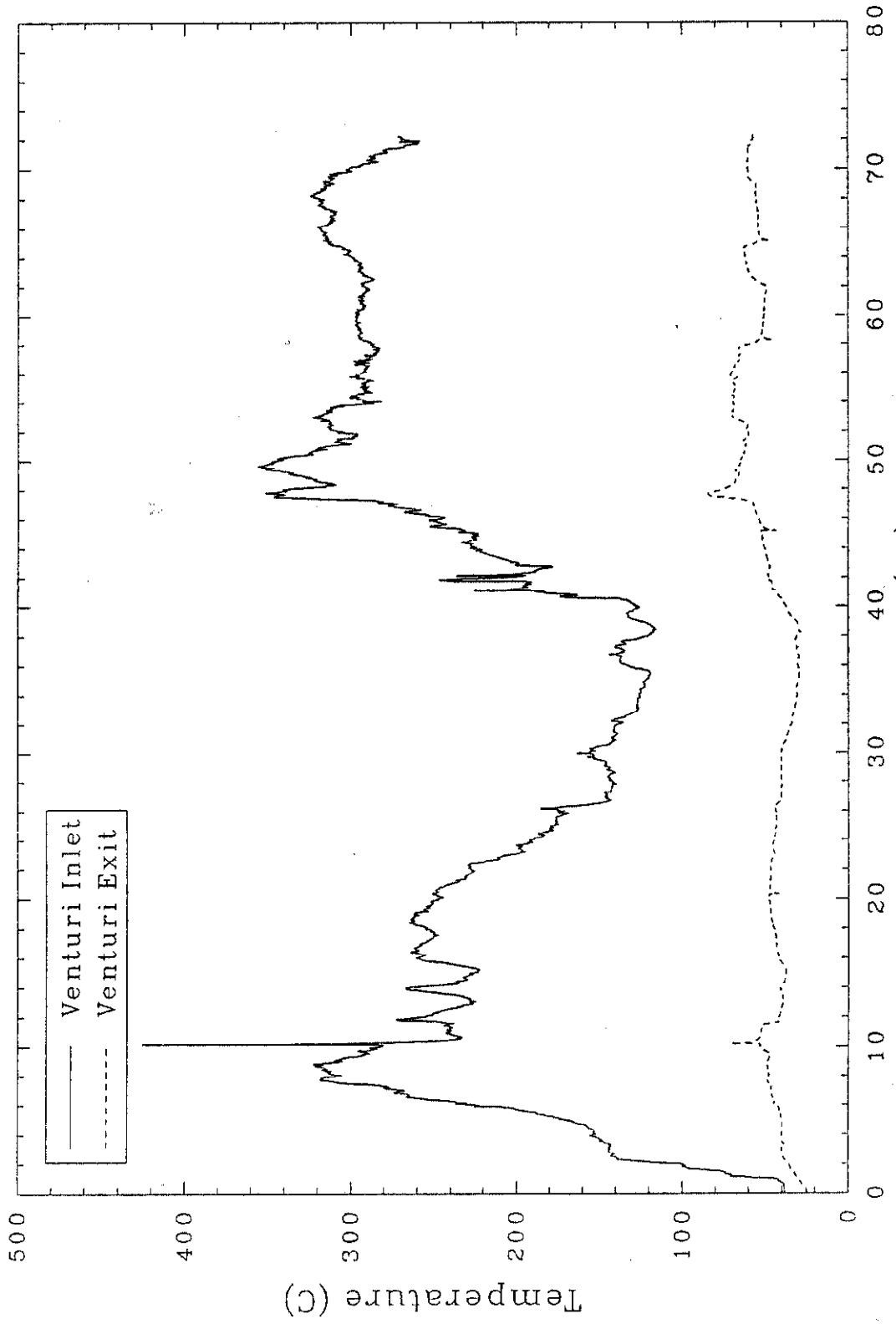


Figure 77. Venturi-Ejector inlet and exit temperatures for Test 2.

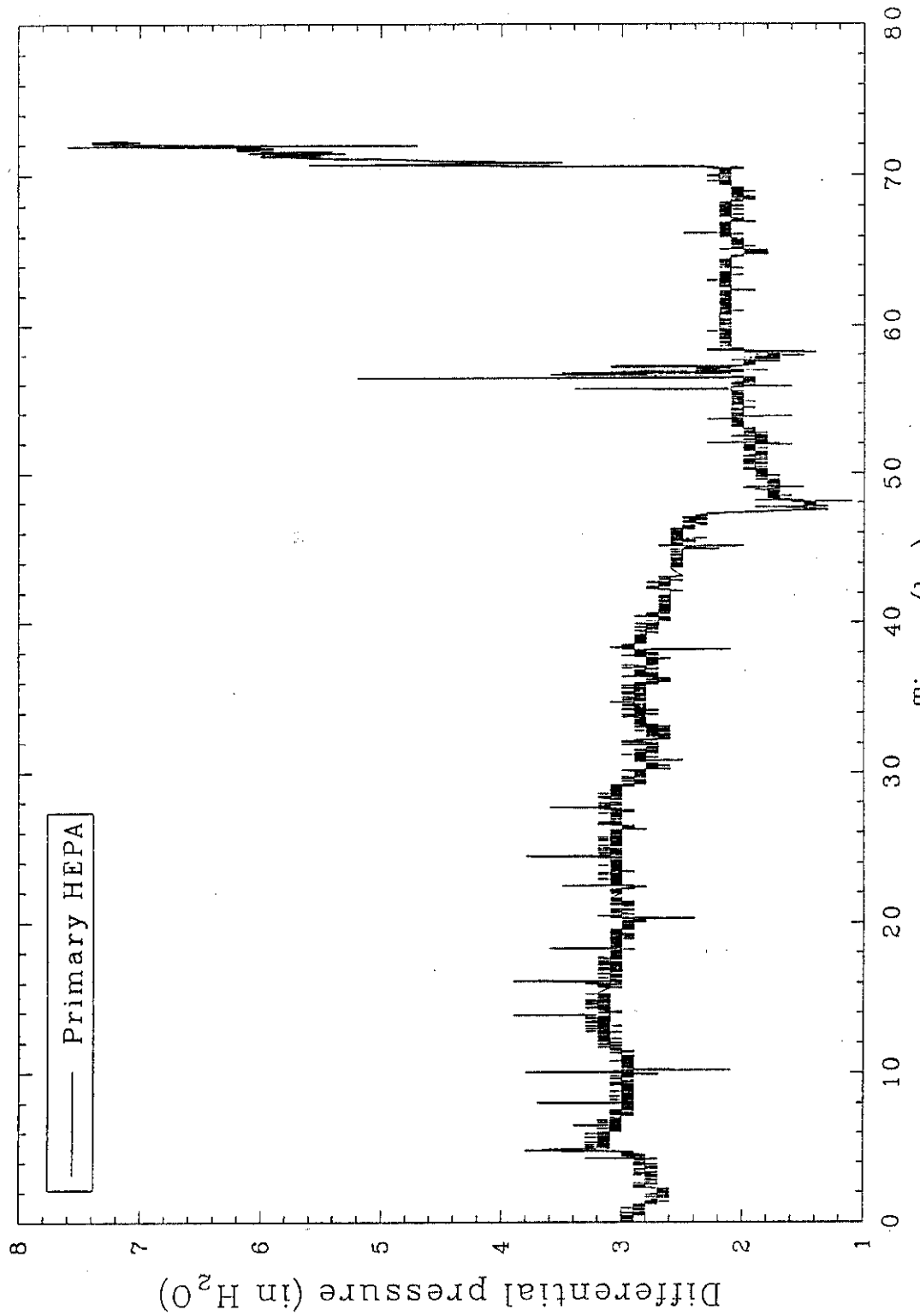


**Figure 78.** Primary HEPA filter differential pressure for Test 2.

spikes at 57 and 71 hours represented a sudden increased differential pressure due to a wet HEPA filter caused by the flooding of scrub solution tank 2. The depth level indicator for tank 2 failed due to the plugging of the small diameter tubing associated with the differential-pressure depth indicating system. The tubing became plugged due to the heavy particulate loading in the off-gas stream and created an inability to ascertain the level of the scrubbing liquid in tank 2. The first wet HEPA was dried by increasing the temperature on the gas heater upstream of the filter. The second wet HEPA occurred at a time immediately prior to the termination of the test, well after electrode power had been terminated.

The plugging of the small diameter tank-level indicator tubing illustrates a larger problem with particulate generation from the test. Relative to a contaminated soil site, the vitrification of a simulated buried waste site apparently results in a greater amount of particulate generation from the melt. The increased levels of particulate generation will require design considerations for a large-scale buried waste ISV machine. The increased amount of particulate in the off-gas stream created two key problems in addition to the small diameter tubing problem mentioned above.

- Solids deposited at the inlet to the Venturi-Ejector resulted in an increased differential pressure across the Venturi-Ejector. This increase in differential pressure is illustrated in Figure 79. The first indication of solids buildup occurred between 30 to 35 hours. Because the differential returned to previous levels, the solids deposit dislodged. Later, at approximately 45 hours, the differential trended more negative, indicating additional solids were depositing at the Venturi-Ejector inlet. The solids deposit created a restricted orifice that reduced total off-gas flow through the system. Upon removal and disassembly of the off-gas line following the test, a large barnacle-like deposit of solids was discovered at the inlet of the Venturi-Ejector.

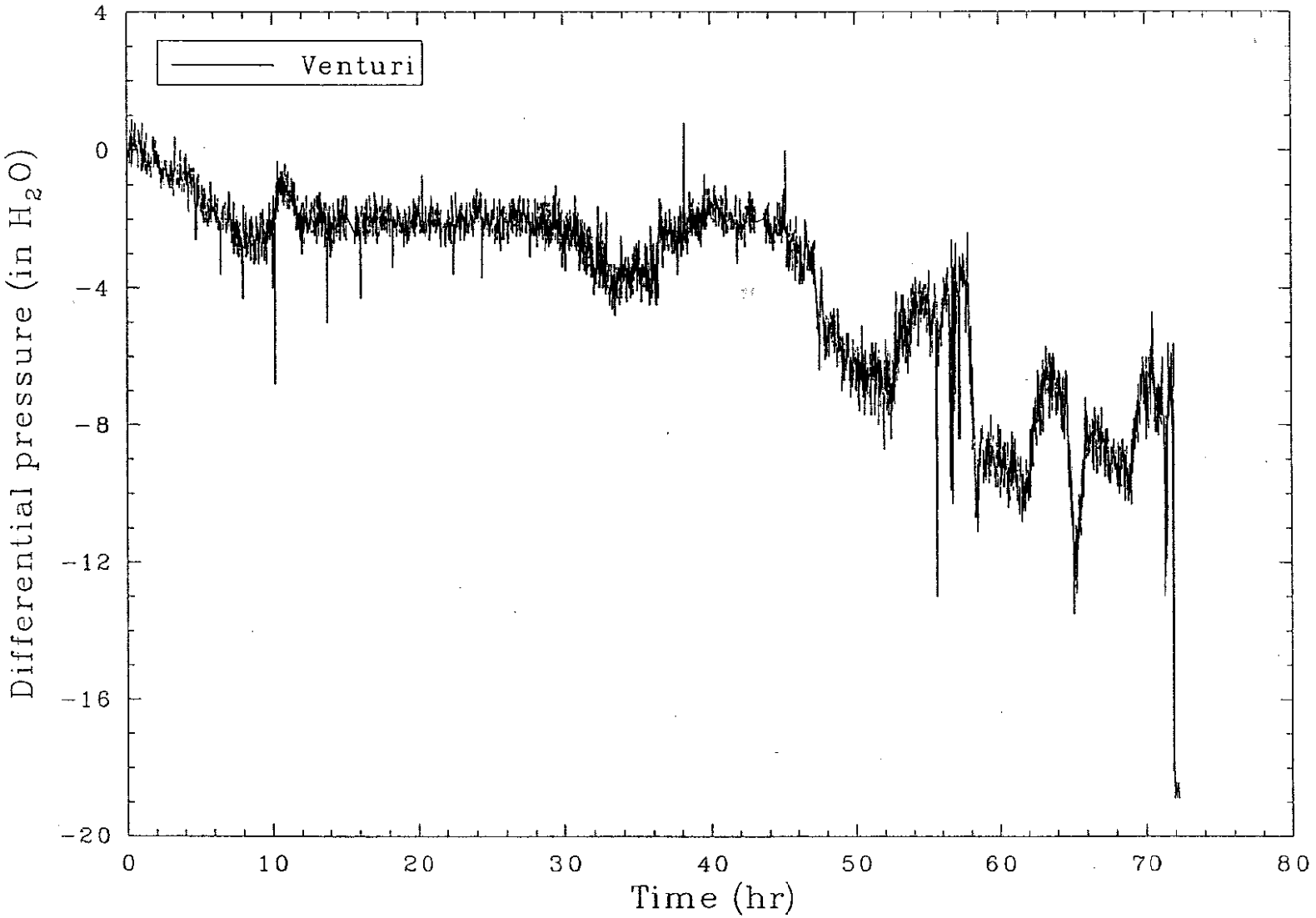


**Figure 79. Venturi-Ejector differential pressure for Test 2.**

- Spray nozzles in the Hydro-Sonic scrubber became partially plugged due to solids in the scrubbing solution. Approximately 50% of all nozzles in each of the two scrubber stages were found to be plugged once equipment was disassembled for inspection following the test. This plugging resulted in an increased pump 2 pressure and a decreased differential pressure across the Hydro-Sonic scrubber, as shown in Figure 80. However, the differential pressure was sustained above 50 in. of water for the test duration except for two short periods at approximately 56 and 58 hours. The average differential would have resulted in an adequate scrubbing efficiency to prevent particulate carryover to the HEPA filters.

Note that because the scrub solution used for Test 2 was the same for Test 1, the solids accumulation in the scrub tanks, nozzles, and small diameter tubing represented the contribution of particulate from two tests. However, the solids accumulation from these tests of simulated buried waste sites is still considered to be excessive based on numerous contaminated soil tests.

The off-gas flow rate averaged 15 $m^3$/min and was more consistent compared to the flow rate in Test 1, shown in Figure 81. The more consistent flow rate was due to the absence of the dramatic pressure spikes that were observed in Test 1 and the new position of the flow sensor upstream of the blower surge protection inlet. Because the off-gas flow was much more consistent with fewer pressure spikes compared to Test 1, the surge protection device remained closed during the vast majority of the test.

The uncoated electrodes performed well. No sticking was observed during the test indicating the difficulties observed in Test 1 were primarily due to the silica-based coating. Oxidative losses were acceptable. One phase A electrode decreased in diameter from 15.2 to 8.9 cm (6 to 3.5 in.) and exhibited a sharp taper over a 17.8 cm (7 in.) region just above the glass level. One phase B electrode reduced in diameter from 15.2 down to 10.2 cm (6 to 4 in.) and exhibited a gradual taper over a 0.6 m (2 ft) length above the glass level. As in Test 1, Test 2 represented a difficult challenge for the

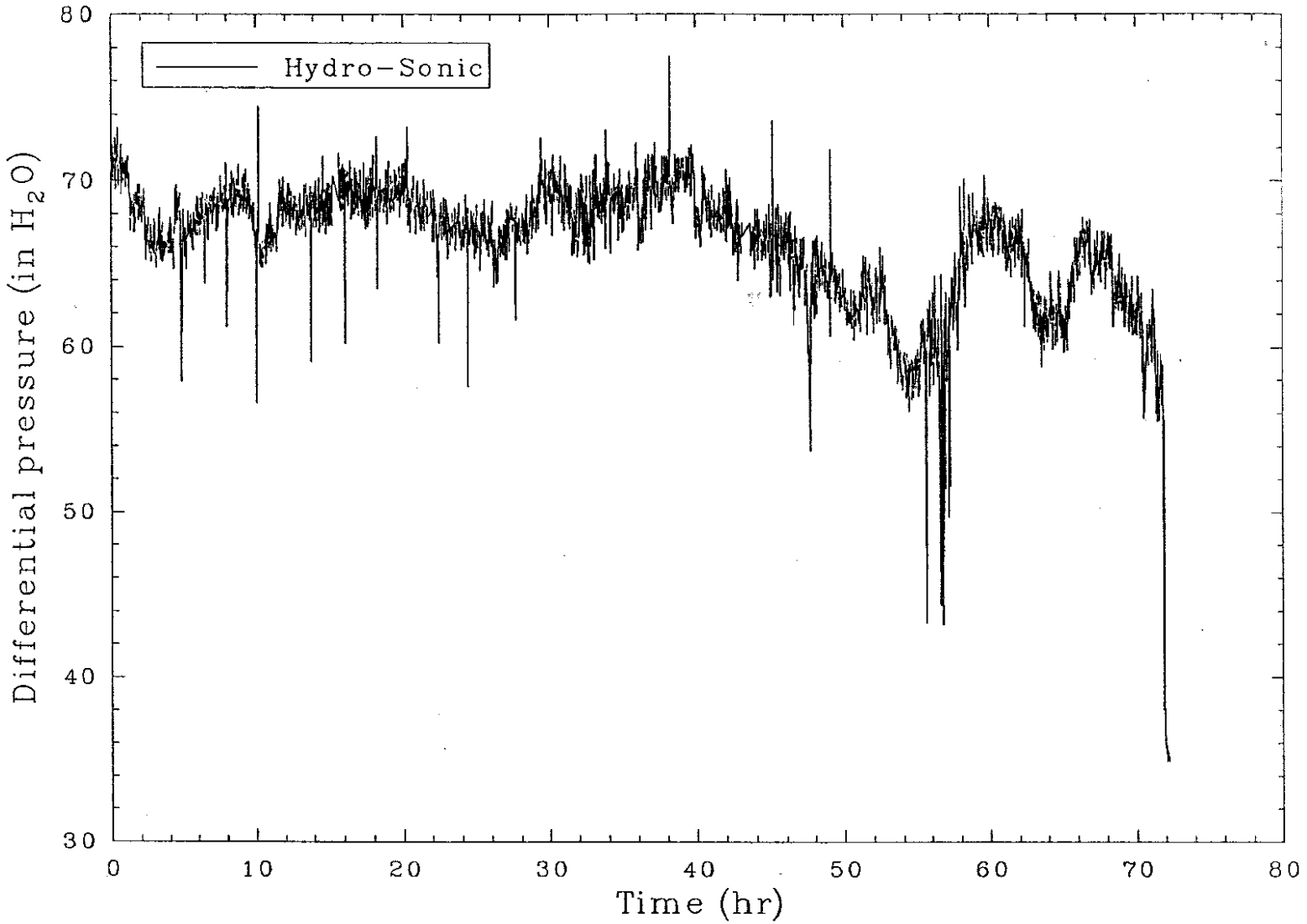


**Figure 80.** Hydro-Sonic differential pressure for Test 2.

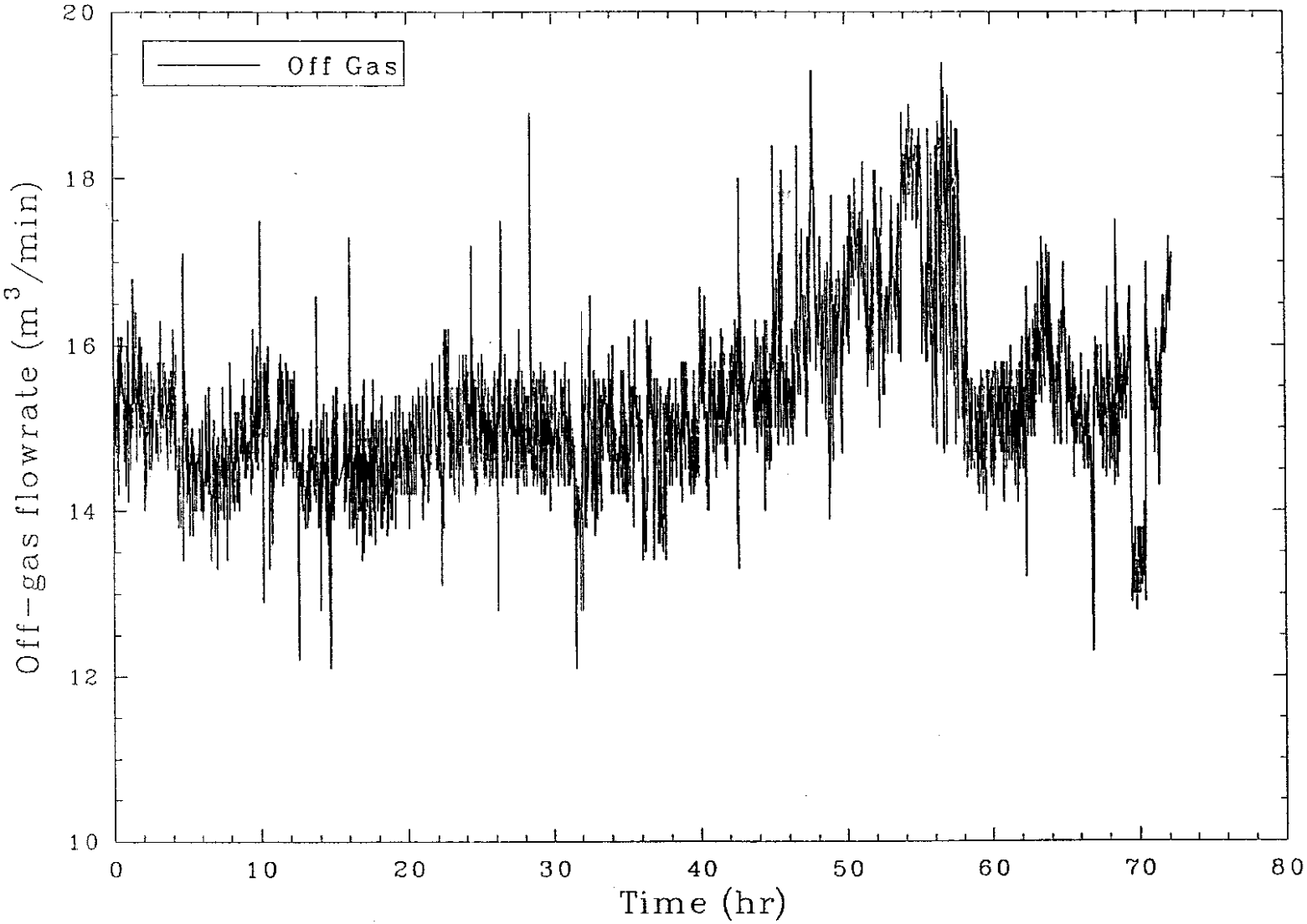


**Figure 81.** Off-gas flow rate for Test 2.

graphite electrodes. Due to the significant amount of subsidence in the melt [measured at 2.3 m (7.5 ft.)], the portion of the electrode at the air/glass interface remained relatively constant throughout the test. Initially, the electrodes were inserted in the soil to a 30.5 cm (12 in.) depth. Consequently, the air/glass interface location relative to the electrodes stayed fairly constant throughout the test. Final glass depth was measured at 0.9 m (36 in.).